energies

MDPI

Review

Exploring Prognostic and Diagnostic Techniques for Jet Engine Health Monitoring: A Review of Degradation Mechanisms and Advanced Prediction Strategies

Maria Grazia De Giorgi *, Nicola Menga and Antonio Ficarella

Department of Engineering for Innovation, University of Salento, Via Monteroni, 73100 Lecce, Italy
* Correspondence: mariagrazia.degiorgi@unisalento.it

Abstract: Maintenance is crucial for aircraft engines because of the demanding conditions to which they are exposed during operation. A proper maintenance plan is essential for ensuring safe flights and prolonging the life of the engines. It also plays a major role in managing costs for aeronautical companies. Various forms of degradation can affect different engine components. To optimize cost management, modern maintenance plans utilize diagnostic and prognostic techniques, such as Engine Health Monitoring (EHM), which assesses the health of the engine based on monitored parameters. In recent years, various EHM systems have been developed utilizing computational techniques. These algorithms are often enhanced by utilizing data reduction and noise filtering tools, which help to minimize computational time and efforts, and to improve performance by reducing noise from sensor data. This paper discusses the various mechanisms that lead to the degradation of aircraft engine components and the impact on engine performance. Additionally, it provides an overview of the most commonly used data reduction and diagnostic and prognostic techniques.

Keywords: EHM; diagnostics; prognostics; data reduction; data-driven methods; model-based methods

Citation: De Giorgi, M.G.; Menga, N.; Ficarella, A. Exploring Prognostic and Diagnostic Techniques for Jet Engine Health Monitoring: A Review of Degradation Mechanisms and Advanced Prediction Strategies. *Energies* **2023**, *16*, 2711. https://doi.org/10.3390/en16062711

Academic Editor: Davide Astolfi

Received: 31 January 2023
Revised: 21 February 2023
Accepted: 8 March 2023
Published: 14 March 2023

1. Introduction

Gas turbines (GTs) convert chemical energy from burned fuels into mechanical power. They use high temperatures and pressures in a combustion chamber to generate thrust, which is necessary for sustained flight. However, these extreme working conditions, including high temperatures, pressures, and rotational speeds, lead to gradual degradation of the turbine's components over time. The degradation of the submachines constituting an aircraft engine leads, in turn, to a reduction in engine performance [1] and flight safety and in an increase in fuel consumption and pollutants. In ref. [2] is presented an estimation model for the prediction of the effect of different forms of degradation on the creep life of gas turbines. Interesting research on the state of the art of aircraft and airport emissions is available in [3]. A maintenance plan is crucial for aeronautical companies. To enhance engine reliability, flight safety, and effectively manage costs, current research efforts are primarily focused on optimizing maintenance plans [4,5]. In the early days of aircraft engines, defects were identified and repaired through Corrective Maintenance (CM). However, this approach was later replaced by Preventive Maintenance (PM), in which inspections and tasks are scheduled according to the probability of failure for specific components and usage conditions. However, less frequent PM reduces safety and more frequent PM increases costs. In [6], concepts such as mean time to failure and mean time between failures are introduced and a study on the effect on the reliability of PM application is conducted. However, because PM is based on probability rather than the actual condition of the components, it can result in non-optimized costs. This approach can lead to the maintenance of components that have not yet reached a critical state, or to the failure of components that have already degraded beyond repair. To optimize maintenance plans, modern approaches such as Condition-based Maintenance (CBM) or predictive

maintenance are increasingly being used in the aviation industry, which take into account the actual condition of the engine components [7,8]. As reported in [9], the implementation of Condition-based Maintenance (CBM) involves three primary stages: data acquisition, data processing, and maintenance decision making. CBM has the potential to reduce maintenance costs by 25−35%, eliminate breakdowns by 70−75%, reduce breakdown time by 35−45%, and increase production by 25−35% [10]. However, a maintenance strategy may be the best for a certain component and the worst for another one [11]. To continuously monitor the condition of engines, appropriate sensors are installed throughout the powertrain to gather useful information. Figure 1 illustrates the different maintenance strategies, and Table 1 provides their characteristics.

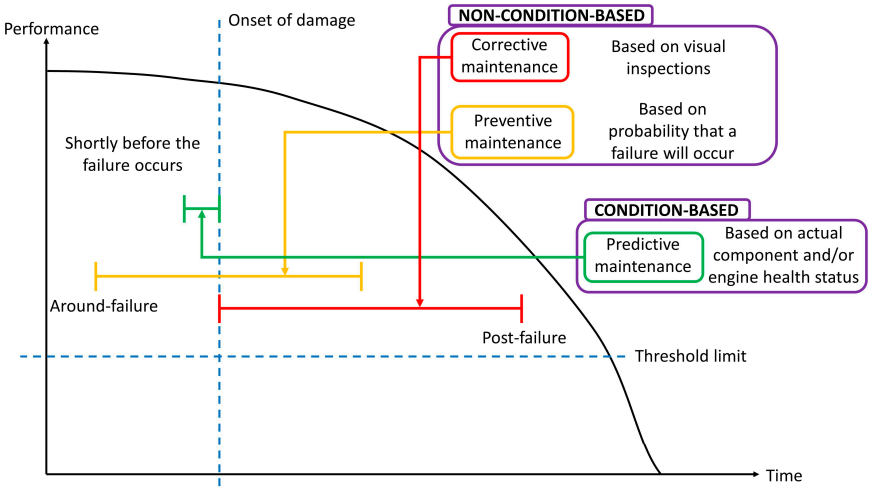

Figure 1. Maintenance strategies illustration.

Table 1. Characteristics of the typical maintenance strategies.

Strategy	Principle	Data Required	Data Analysis	Maintenance Decision	Related Problems	Refs.
CM	Reactive-based; Unscheduled; Fail and fix approach.	No data measurements are required. Corrective maintenance is based on visual inspections.	No data to analyze.	Maintenance is performed only after a detected failure by a visual inspection.	Faults cannot be predicted and are not avoided by scheduled maintenance; Higher maintenance costs; Lower reliability compared to other maintenance strategies.	[4,12,13]
PM	Time-based; Scheduled. Maintenance interval depends on the probability of failure occurring; Preventive approach.	Historical data on components failure or test data.	A reliability theory based on bathtub curve assumptions.	Maintenance is performed after predetermined time intervals, obtained from statistical analysis of available historical data about failure of components or test data.	The maintenance plan is based on statistical assumptions. A component could be overhauled even if in good condition or could be subject to a fault before being overhauled; Higher maintenance costs and lower reliability compared to the predictive strategy.	[5,6,12,13]
CBM	Condition-based; Just-in-time. Maintenance interventions request only when necessary; Preventive and predictive approach.	Information about actual values of some parameters used as health indicators of the components (temperatures, pressures, etc.).	Monitoring the component state of health.	Maintenance is performed when monitored parameters indicate an impending failure in one or more components.	More complex approach; Require more efforts and time for strategy development.	[5,7–10,12,13]

The engine's performance is contingent on the performance of its individual components, which can be evaluated using parameters such as temperature, pressure, rotational speed, torque, and fuel flow. Additionally, the presence of contaminants in oil and exhaust gases, or high levels of vibration and noise from the components, may also indicate deteriorating performance [14]. For example, Blade Tip Timing (BTT) is a non-contact measuring

technique commonly used today to monitor the strains and vibrations of blades. This technique addresses some of the limitations of strain gauges [15], such as the inability to use them on in-service engines because they need to be affixed to the blade airfoil. In BTT, sensors are typically mounted on the casing to detect the vibrations of the blades as they pass by [16]. The BTT technique serves as the foundation for a proposed method to detect crack propagation in rotor blades, as described in [17] This method involves monitoring the natural frequencies of cracked blades and comparing them to those of a healthy blade. In [18], a method that utilizes the BTT technique for dynamic strain reconstruction in rotating blades experiencing multi-mode vibration is presented. Dynamic strain measurement is essential for monitoring the health status of rotating blades [19]. However, the BTT technique can encounter certain issues. Mohamed et al. [20] propose an improvement of the technique. Computer algorithms are commonly used for diagnostic and prognostic tools, which are the key components of CBM. In recent years, the concept of biomimicry has been gaining momentum, driving the development of improved algorithms and materials that draw inspiration from nature itself [21,22]. Diagnostics involves determining the current condition of a system based on sensor-provided data on its physical parameters. Prognostics, on the other hand, focuses on predicting the remaining lifespan of a system using historical and current data on its condition, which are also collected by sensors. These topics will be further explained and illustrated with examples in the following sections. Section 2 of this paper covers the main degradation phenomena that affect gas turbines and their impact on engine performance. Section 3 focuses on the data acquisition and processing stage, including methods for reducing data dimensionality and noise. Section 4 provides an overview of the commonly used diagnostic and prognostic techniques. Finally, Section 5 concludes the review and offers suggestions for future research. Currently, many studies are being conducted on diagnostic and prognostic systems for aircraft engines, and examples can be found in the literature in [23–28].

2. Degradation Mechanisms of an Aircraft Engine

Aircraft engines, like any machine, experience degradation over time. Compressors and turbines are particularly vulnerable to degradation, which can manifest in various forms. The occurrence of degradation is a random event influenced by factors such as the operating environment [29] and type of mission (e.g., high- or low-power requirements), with unexpected events such as collisions with objects also playing a role.

Research on the impact of the operating environment on degradation can be found in [30,31]. In particular, the study reported in [30] describes two experiments in which sand is intentionally introduced into the inlet of an aircraft engine. In the first experiment, a substantial quantity of sand is rapidly introduced, while in the second, the amount of sand injected simulates what an engine would experience in real-world conditions. Both experiments result in a decrease in thrust and an increase in fuel consumption per unit of thrust. In [31], computational fluid dynamics is utilized to investigate the corrosive effect of volcanic ash on fan blades, using two different methodologies: one that assumes a constant rate of erosion and the other that adapts the erosion rate. The simulations in both cases demonstrate that erosion is more severe moving from the midspan towards the tip. On the suction side, the most significant loss of material is concentrated around the leading edge in the vicinity of the hub and extending towards the midchord for the outer midspan sections. On the pressure side, the material removal is less severe and primarily located near the midchord of the tip. The most prevalent forms of degradation are fouling, erosion, corrosion, and an increase in blade tip clearance. Severe but random events such as collisions with objects from the external environment or the engine itself can also occur. The impact of degradation on components results in a decline in performance, as evidenced by changes in Performance Parameters (PPs), which are all operating parameters that are influenced by the condition of the parts and impact engine thrust and fuel consumption [32]. Changes in non-measurable PPs can lead to deviations in measurable PPs that are dependent on the

former, which can serve as an indicator of the engine's health. Table 2 provides a summary of the PPs commonly used for both stationary and aircraft engines.

Table 2. Commonly used PPs for aeroengines [32].

Performance Parameter	Metric Unit	Engine Type
	Measurable *	
Exhaust gas temperature (EGT)	°C	Aero jet engines
Fuel flow	kg/s	All types
High-pressure spool speed	RPM	Aero jet engines
Low-pressure spool speed	RPM	Two-spool GT
Intermediate-pressure spool speed	RPM	Three-spool GT
Compressor outlet pressure	kPa	Aero jet engines
Compressor outlet temperature	°C	Aero jet engines
Turbine inlet temperature	°C	Aero jet engines
Torque	Nm	Turboshaft/Turboprop
Component vibration	m/s^2	All types
	Estimated *	
Power	kW	Piston engine/APU
Thrust	kN	Aero jet engines
Specific fuel consumption	Kg/kJ	Piston engine
Thrust specific fuel consumption	g/(kN·s)	Aero jet engine
Air flow	kg/s	All types
Exhaust gas flow	kg/s	Aero jet engines
Exhaust gas velocity	m/s	Aero jet engines
Heat rate	kJ/kWh	All types
Thermal efficiency	%	All types

* Measurable: Parameters obtainable by means of adequate sensors; Estimated: Parameters computed starting from the measurable ones.

For compressors and turbines, flow capacity and efficiency are commonly used as PPs. These parameters are not directly measurable, but they influence the inlet and outlet temperatures and pressures of the same components [33]. A degraded state can also be diagnosed by monitoring other characteristics, such as component vibration and noise, or the presence of debris in the oil and gas path [32,34–38]. A description of the main degradation mechanisms mentioned above follows.

2.1. Fouling

Fouling is the adhesion of contaminants present in the operative flow on the surfaces of components, such as dust, sand, dirt, ash, oil droplets, water mists, hydrocarbons, and industrial chemicals [39]. Due to their position in the gas path, compressors are the components most affected by fouling. In addition, compressor fouling is the most common degradation problem [40] and is usually caused by particles smaller than 2 to 10 microns [41]. The adhesion of dirt particles on the surfaces leads to a change in the aerodynamic shape and inlet angle of the airfoil, an increase in roughness, and a decrease in the opening of the airfoil [42,43], resulting in a decrease in efficiency, flow capacity, and pressure ratio [44]. The consequence on the overall GT is a decrease in output power and thermal efficiency [40]. Some of the power loss caused by compressor fouling can be recovered by washing [45,46]. The three main types of washing systems, i.e., on-line washing system, off-line crank washing system, and manual hand crank washing system, are described in [47]. Fouling has a greater effect on the first compressor stages, while it is limited in the backward stages [48,49]. Experiments conducted by Kurz et al. [50] show that the amount of dust picked up by the blades varies depending on their surface characteristics. In [49], an analytical method is proposed for investigating the fouling phenomenon in the axial compressors of industrial gas turbines. The results reveal a relationship between the axial compressor and flow characteristics, such as chord length, solidity, number of stages, particle size, flow rate and inlet flow angles, and the fouling phenomenon. Specifically, the authors of the study conclude that the number of particles adhering to the blades increases with decreasing chord length and an increase in solidity, fouling accelerates with decreasing flow rate and inlet flow angle, and fouling is more prevalent in the forward stages. Some

examples of the effects of fouling on different GTs are given below. In [40], a simulation was conducted in which there was a 6% reduction in mass flow and a 5% decrease in compressor efficiency, resulting in a 55 kW drop in power and an increase of 850 Btu/kW hr in heat rate. Additional simulation results are also provided in the same study. A 5% decrease in flow capacity and 2.5% decrease in compressor efficiency results in a 10% reduction in output power [51]. A decrease of 7% in output power, accompanied by a 2.5% increase in heat rate, results from a 5% decrease in compressor inlet mass flow rate and a 1.8% decrease in efficiency, as reported in [42]. In [48], a decrease in stage pressure ratios is shown with an increase in operating hours for different compressor stages. Figure 2, taken from [52] (a and b) and from [53] (c), shows some examples of fouling. In detail, in Figure 2a,b is visible the fouling phenomena on Low-Pressure Compressor (LPC) stage blades and on Low-Pressure Turbine (LPT) vane, respectively, while in Figure 2c shows deposits of volcanic ash on the High-Pressure Turbine (HPT) nozzle guide vanes.

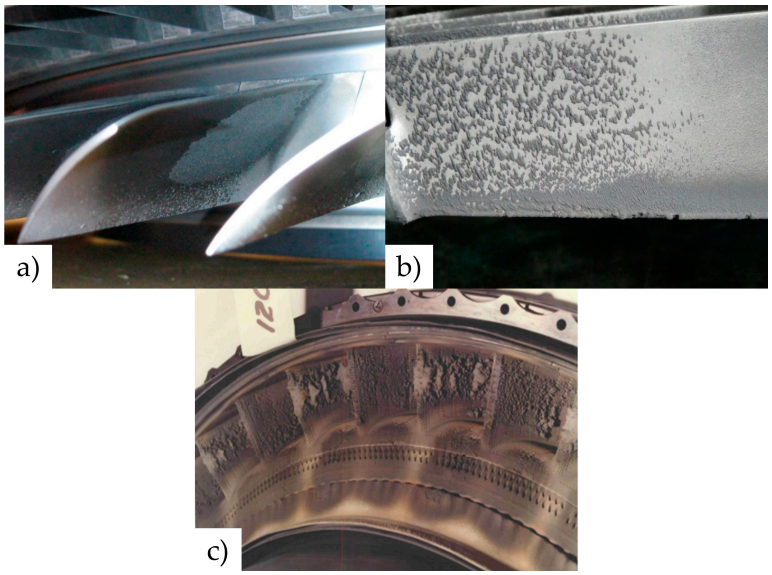

Figure 2. Some examples of fouling verification [52] (**a**,**b**), [53] (**c**). (**a**) Deposits on LPC blade; (**b**) Deposits on LPT vane; (**c**) Deposits of volcanic ash on the HPT nozzle guide vanes.

2.2. Erosion

Erosion is the gradual loss of material from the gas path due to impact with hard particles that contaminate the operational flow, such as sand, dust, dirt, ash, carbon particles, and water droplets. Unlike fouling, in erosion, the interaction between larger particles of contaminants and blades causes the latter to lose a small portion of material. This leads to a change in the aerodynamic shape and roughness, and reduces performance [54]. More in detail, erosion causes a drop in efficiency and flow capacity in an affected compressor, while manifests itself in turbines causing a decrease in efficiency and an increase in flow capacity [55]. On the overall GT, erosion leads to a decrease in output power and an increase in heat rate [42]. Otherwise, the breaks on the blades create stress concentration zones, which reduces fatigue strength. Despite the fact that erosion can occur anywhere in the gas path, turbines are more susceptible to this phenomenon than compressors [39]. Erosion is a problem most commonly encountered in aircraft engines than in industrial ones, due to more effective filtration systems used in this latter environment [56]. In [57], erosion in turbomachinery is predicted by means of an analytical model developed in the same paper. Furthermore, at the end of the study, the authors conclude that, in general, in an axial flow compressor, erosion manifests itself by cutting back the leading edge and thinning the trailing edge of the blade. They also state that, especially after impacting a rotor, particles will centrifuge radially, concentrating on the tips of the blades and causing severe damage in this location. Erosion damages can be reduced by applying a coating

on compressor and turbine blades, in order to protect them from the impact of hard and large contaminants particles which cause erosion. In [58], the protective capabilities against erosion and corrosion on compressor blades of various coatings are investigated. The results conclude that coatings obtained by physical vapor deposition show the best results in both erosion and corrosion protection, particularly the (Ti, Al)N coatings. Electron beam physical vapor deposition thermal barrier coatings have been used for protection purposes for several years, and more studies on their erosion and corrosion mechanisms and resistance have been conducted [59–62]. More information on coatings and erosion are reported in [63–69]. Figure 3, taken from [52], portrays the erosion effect on the leading edge of fan blades.

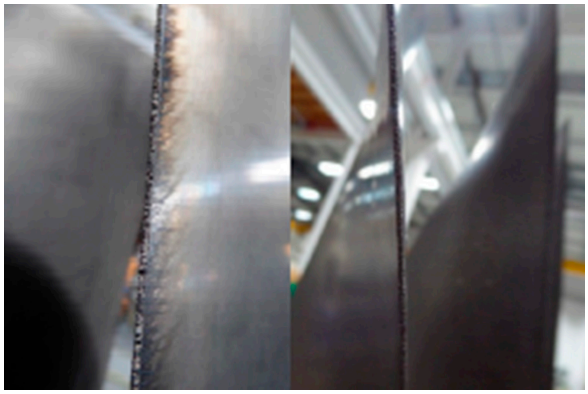

Figure 3. Example of erosion phenomenon on the leading edge of fan blades [52].

2.3. Corrosion

Corrosion is a chemical reaction between some reactive particles contained in the operational flow and the material that constitutes the components encountered in the gas path. "Cold corrosion" refers to the corrosion reaction that occurs in compressor sections, due to wet deposits of salts, acid, and aggressive gases such as chlorine and sulfides. On the other hand, the corrosion occurring in the turbine is known as "hot corrosion," which is a form of accelerated oxidation caused by molten salts that chemically react with the surfaces of the components on which they rest. Hot corrosion is further dividId into two classes: high-temperature hot corrosion (or type I) that occurs at a temperature range of 730 to 950 °C, and low-temperature hot corrosion (or type II) that occurs at a temperature range of 550 to 730 °C [70]. More information is available in [71]. Corrosion is one of the main reasons for blade failure [72]. A series of examples of aircraft failures due to corrosion are available in [73], as well as further information on the phenomenon of corrosion. RD-33 turbofan engine is presented in [74], and the effect of corrosion on it is shown. In [75], eddy current testing is presented as a means of detecting defects resulting from corrosion around the rivets of supersonic aircraft intakes. As reported in the paper, this type of corrosion is caused by the presence of moisture and salinity in the atmosphere, and eddy current testing is a more suitable technique for detecting deeper defects. Corrosion is a phenomenon that must be carefully monitored, as it can result in significant cost increases. Today, various non-destructive techniques are used to detect ongoing corrosion processes [76]. Also for corrosion, compressor and turbine blades can be protected by means of adequate coatings [77]. The effect of corrosion on the compressor is a decrease in efficiency and flow capacity, while on the turbine, corrosion leads to a decrease in efficiency and an increase in flow capacity [78], resulting in a decrease in engine performance. In Figure 4, taken from [52], are visible the effects of corrosion on an LPT vane.

Figure 4. Corrosion effect on a LPT vane [52].

2.4. Abrasion

Abrasion is a loss of material due to the rubbing of one surface against another. The removed material typically leads to an increase in seal or tip gaps. Minimizing clearances between blade tips and casing is crucial for reducing the aerodynamic losses that occur in rotating machines, as the overall engine efficiency is negatively impacted by these losses [79]. In many cases, abradable surfaces are present. In these engines, a certain amount of rubbing is allowed during the run-in of the engine to establish proper clearances [80]. In [81], a study is conducted to investigate the high-speed scraping behavior between a vulcanized silicone rubber and a Ti-6Al-4V fan blade. Blade tip rubbing can occur due to an unbalanced or misaligned rotor due to the shaft bearing damage, engine rotor flexing at heavy operating loads, or the thermal growth of blades [82]. The result is an increase in blade tip clearance. Another phenomenon that leads to tip rubbing is the engine casing distortion due to flight loads. The principal effect of this is a reductIon in the efficiency of the damaged component [78], which results in a drop in engine performance. An example of abrasion on a High-Pressure Compressor (HPC) blade is depicted in Figure 5, taken from [52].

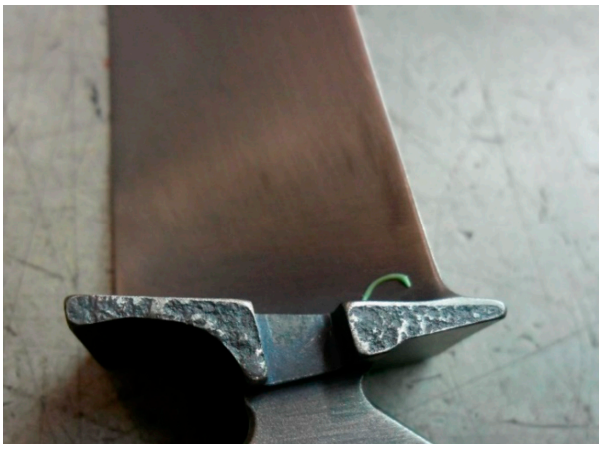

Figure 5. Effect of the abrasion mechanism on a HPC blade [52].

2.5. Thermal Distortion

Thermal distortions typically occur at combustor exit and are due to some problems located in the previous stations, such as the cocking of fuel nozzles, change in fuel spray angles, change in compressor performance, and warping of the combustor liners, which in turn result in a change in radial and circumferential temperature patterns at the combustor exit. The results could be temporary or permanent damage in the downstream components,

such as crack, bending, warp, burn in turbine nozzle guide vanes, and change in nozzle guide vanes areas. The principal effect is a drop in turbine efficiency [26,78], which is responsible for a reduction in engine performance. Figure 6, taken from [52], reports a burned HPT blade.

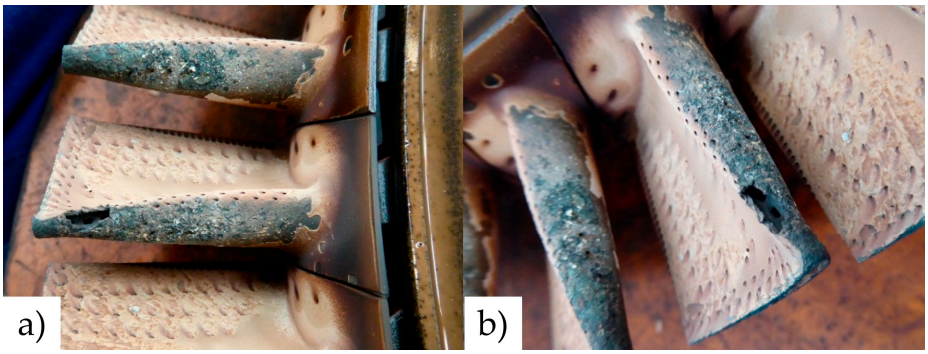

Figure 6. A burned blade at HPT [52].

2.6. Foreign Object Damage and Domestic Object Damage

Foreign Object Damage (FOD) and Domestic Object Damage (DOD) refer to damage caused by impact with objects from the external environment and from the GT itself, respectively. For example, FOD can be caused by impact with ingested birds, ice, stones, debris, and gravel on runways, while DOD can be caused by impact with fragments detached from blades or large carbon particles from the fuel nozzles [39]. FOD and DOD damages are comprised between nonrecoverable (with washing) fault and a catastrophic engine fault [42]. FOD is one of the biggest problems and can lead to catastrophic failures [83]. The effects on performance primarily focus on the efficiency variation of the affected component. The changes in flow capacity depend on how the objects causing the FOD/DOD interact with the component. If the impact results in a lost blade, flow capacity increases, while if the object gets stuck and obstructs the flow, flow capacity decreases [78]. The cases shown in Figure 7, both taken from [52], depict damage that is typically due to the impact with a sharp object (a) and the breaking of a blade of a HPC (b).

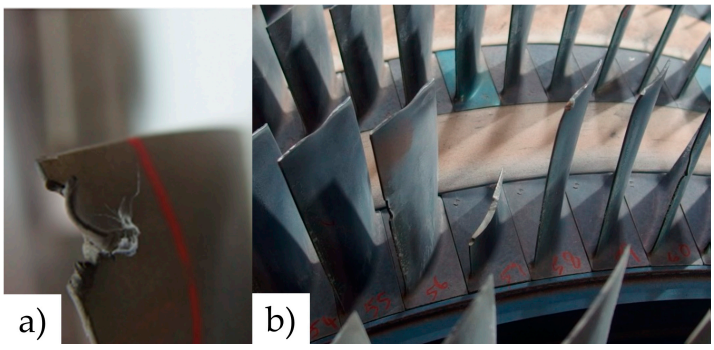

Figure 7. Possible damages due to impacts [52]. (**a**) Impact with a sharp object; (**b**) Broken HPC blade.

2.7. Increased Blade Tip Clearance

Due to phenomena that can remove material, such as erosion, impact with contaminants, or thermal and centrifugal expansions, the clearance between moving blades and stationary blades with casing and a rotating hub, respectively, increases [33,84]. The power elaborated by the compressor and turbine depends on the amount of air flowing through the area occupied by blades, so the increase in blade tip clearance results in more flow passing through the compressor and turbine sections without being processed by the stage, resulting in a decrease in the efficiency of the rotating machine [85]. Stall margin is also affected by an increase in blade tip clearance in axial compressors [86]. An increase in blade

tip clearance of about 0.125 mm in HPC or HPT can reduce the related efficiencies by 0.5%. Furthermore, an increase in engine specific fuel consumption by 0.2% and 0.25% is present when HPC is affected and when HPT is affected, respectively [87]. Other examples show a reduction of 3% and 2% in flow capacity and isentropic efficiency, respectively, due to an increase in tip clearance of 0.8% [88]. In [89], the results of experiments on the effect of compressor rotor tip clearance on the performance of a turboshaft engine are reported. The experiments were conducted on a combined five-stage axial and one-stage centrifugal compressor. Specifically, the experiments were conducted by simulating an increase in tip clearance, first only at the first axial stage, and subsequently, only at the fifth axial stage for different severity levels in both cases; then, finally simulating equal damage severity at all five axial stages simultaneously. All the experiments show a reduction in overall engine performance. In more detail, the results show that a small increase in tip clearance throughout all stages is responsible for a greater loss in performance than a larger increase in tip clearance at only one stage. A further study on the effect of increased blade tip clearance has been conducted by Gourdain et al. where three different configurations were considered for a multi-stage high-pressure compressor, one of which considered a casing treatment based on a honeycomb design. More information is available in [90]. The increase in blade tip clearance has a significant impact on the aero-elastic stability of the blades, which is an important aspect that cannot be ignored. The reason for this is the profound impact that aero-elastic phenomena have on blade health status and, consequently, engine performance. Aero-elastic phenomena such as flutter and forced vibration, which are caused by the interaction between unsteady aerodynamic forces and blade motion, or by upstream and downstream vane wakes or inlet distortion, respectively, can lead to high cycle fatigue and fractures [91]. In [92], the correlation between the flow of tip clearance and the behavior of another aero-elastic phenomenon called non-synchronous vibration is investigated. Non-synchronous vibration manifests itself similarly to flutter, but it occurs in a region that is far removed from it. In extreme cases, non-synchronous vibration can also result in blade loss [93]. An interesting work is present in [94], in which experiments were conducted to excite aero-elastic phenomena, such as blade forced response, flutter, and acoustic resonance, on an aero-engine's fan. Acoustic measurements were used as a means of recognizing the presence of a particular aero-elastic phenomenon through the appropriate acoustic features. Interested readers can find additional information on blade tip clearance and the technologies used to measure it in [85,95]. A damaged tip (together with the effect of erosion) is visible in Figure 8, taken from [96].

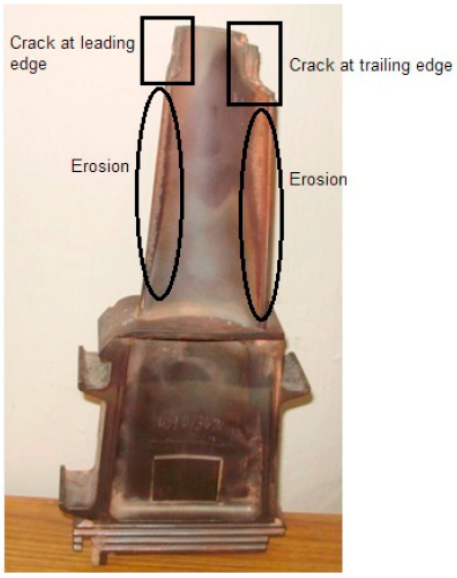

Figure 8. A damaged tip [96].

2.8. Summary of Degrading Phenomena

Table 3 summarizes the degradation phenomena described earlier, along with the effects on the affected components and on the overall GT, based on data available in the literature.

Table 3. Collection of the main degradation phenomena with their effect on the GT. Information found in the literature.

Phenomenon	Mechanism	Exposed Parts	Effects on Parts	Effects on Performance Parameters of Parts	Effects on Engine Performance	Refs.
Fouling	Contaminant particles adhesion on surfaces and blades.	Compressors and turbines. Mainly the compressors.	Change in aerodynamic shape and inlet angle of airfoils; increase in surface roughness and decrease in airfoil throat opening.	Fouled compressor: decrease in η_c, f_c and β_c; Fouled turbine: decrease in η_t and f_t.	Drop in output power and thermal efficiency and increase in heat rate.	[39–51]
Erosion	Loss in material from gas path due to impact with harder and bigger contaminant particles.	Compressors and turbines. Mainly the turbines.	Change in the aerodynamic shape of blades. Increase in roughness and decrease in cross-sectional area.	Eroded compressor: decrease in η_c, f_c and β_c; Eroded turbine: decrease in η_t and increase in f_t.	Drop in output power and increase in heat rate.	[39,42,54–69]
Corrosion	Loss of material in gas path due to chemical reactions between gas-path materials and contaminants.	Compressors and turbines. Cold corrosion is relevant in compressors. Hot corrosion is relevant in turbines.	Change in the aerodynamic shape of blades. Increase in roughness.	Corroded compressor: decrease in η_c and f_c; Corroded turbine: decrease in η_t and increase in f_t.	Drop in output power and increase in heat rate.	[70–78]
Abrasion	Loss in material due to a component rubbing on another one.	Compressors and turbines.	Increase in seal and tip gaps.	Abraded compressor: decrease in η_c; Abraded turbine: decrease in η_t.	Drop in output power.	[78–82]
Thermal distortion	Damages in parts located at burner exit due to a change in radial and circumferential temperature patterns.	Burner exit/ turbine inlet.	Generation of cracks, bends, warpings, burns in turbine nozzle guide vanes and change in nozzle guide vanes areas.	Decrease in η_t.	Drop in output power.	[26,78]
FOD/DOD	Impact with an ingested object or with detached ones from engine components, respectively.	Compressors and turbines.	Bends and breaks in blades.	Affected compressor: decrease in η_c and increase or decrease in f_c; Affected turbine: decrease in η_t and increase or decrease in f_t.	Drop in output power, increase in heat rate.	[39,42,78,83]
Increase in blade tip clearance	Increase in clearance between moving blades and stationary blades with casing and rotating hub, respectively.	Compressors and turbines.	Tip breaks and consequent increase in clearance.	Affected compressor: decrease in η_c and f_c; Affected turbine: decrease in η_t and f_t.	Drop in output power and increase in heat rate.	[33,84–95]

3. Data Acquisition and Processing

The methodologies for prognosis and diagnosis are based on a set of information that assesses the health of an engine and/or its components. In an aircraft engine, various data can be collected in real time to inform diagnostic or prognostic algorithms, such as pressures and temperatures at the inlet or outlet of compressors, turbines, and burners, fuel flow, shaft speed, or torque. To accomplish this, appropriate sensors must be installed throughout the engine. To enhance the performance of the diagnostic or prognostic system, the collected data can be analyzed to eliminate noise measurements, disregard measurements from faulty sensors, and discard redundant information that unnecessarily increases the dataset. This section introduces the concept of data cleaning and provides examples of data reduction techniques used.

3.1. Sensor Measurements

Sensors are the tools used to collect crucial information about the engine's health and the status of its components and subsystems [97]. The use of sensors is very important to

increase flight safety, and good knowledge in this field is fundamental to obtain a modern and safe engine [98]. Sensors are distributed not only in the engines but throughout the entire aircraft. Modern aircrafts have hundreds or even thousands of sensors [99]. Choosing which sensors to install is not a trivial task, and performing a thorough analysis to understand the advantages of various sensors can greatly aid in the decision-making process [100]. Like all other components, sensors can experience faults. A faulty sensor will supply incorrect data to the diagnostic or prognostic algorithm, which may subsequently lead to an inaccurate assessment of the engine's health. To enhance the performance of the EHM system, processing the data obtained from the sensors can be beneficial. For example, in [101], a sensor Fault Detection, Isolation, and Identification (FDII) technique was developed to detect the presence of single or multiple sensor faults. Another noteworthy study was conducted by Sadough Vanini et al. [102], in which they developed an FDII model that handles various degradation scenarios, accounts for concurrent and sensor faults, and is able to rectify erroneous readings from a faulty sensor using the readings of the remaining functional sensors. A similar but older work is presented in [103]. Sensor measurements are also affected by noise and bias, which can increase over time due to sensor aging [104]. Signal filtering or smoothing are helpful approaches to improve the quality of information provided by sensors. Figure 9 illustrates the difference between two different approaches.

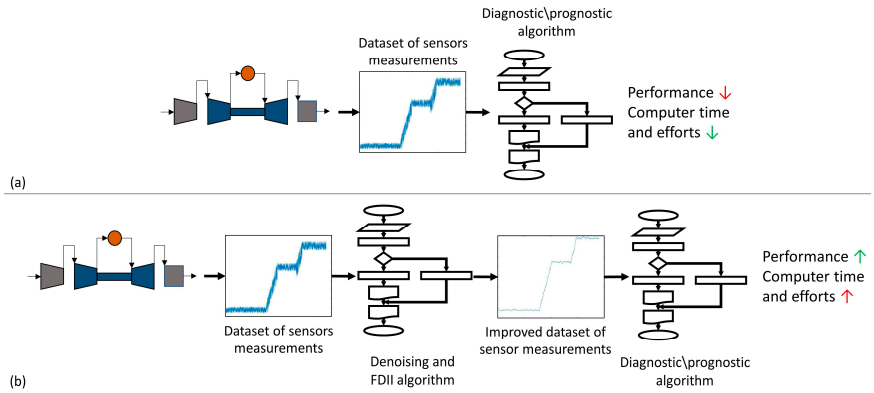

Figure 9. Difference between two approaches: (**a**) Diagnostic/prognostic algorithm informed with pure sensor measurements; (**b**) Diagnostic/prognostic algorithm informed with improved sensor measurements.

Signal denoising is a very active area of research [105]. As reported in [106], the presence of noise in a sensor measurement can be modeled as follows:

$$y_M(t) = y_T(t) + x(t) \tag{1}$$

where $y_M(t)$ denotes the measured noisy signal, $y_T(t)$ denotes the true signal, and $x(t)$ represents the sum of all the noise present in the measurement. For more detailed information on sensor noise, the interested reader is referred to the same paper. A technique employed for noise reduction is the wavelet transform [107,108]. The wavelet transform technique is capable of expressing a given signal as a linear combination of basis functions called wavelets. Wavelets are obtained starting from a base wavelet $\Psi(t)$ called the "mother wavelet", by scaling and translation:

$$\Psi_{(a,b)}(t) = \frac{1}{\sqrt{a}}\Psi\left(\frac{t-b}{a}\right); \quad a, b \in R; a \neq 0; \tag{2}$$

where a is the scale factor and b is the translation factor. Further details on wavelet theory are available in [109].

3.2. Data Reduction Techniques

Diagnostic and prognostic algorithms process a large amount of data from the engine, which contains information about certain monitored parameters used to assess the condition of the components. To improve performance in terms of required computer memory, time, and effort, it is beneficial to analyze the data and use appropriate data reduction techniques to reduce the dataset size [110–112]. In this section, some techniques used to perform a data reduction process, learned from [112], are presented. The notation used in the description of the data reduction methods is the same used in [112], from which information was mainly taken and is reported in Table 4 for simplicity.

Table 4. Notation adopted in the description of the following data reduction methods [112].

Notation	Definition
PC	Principal component
X	Input dataset in high dimension
Y	Output dataset in low dimension
d	Original high dimension
k	New low dimension
x_a	ath input data in d dimension
x_b	bth input data in d dimension
y_a	ath output data in k dimension
y_b	bth output data in k dimension
K	Kernel function
c	Nearest neighbors for a data point
n	Number of data points
i	Number of iterations

3.2.1. PCA

Principal Component Analysis (PCA) is an unsupervised, linear transformation algorithm that produces the so-called Principal Components (PCs) (which represents the new features) based on the variance of the data. The PCA algorithm works by projecting the highly dimensional dataset into a new subspace in which the orthogonal axes, the PCs, represent the direction of the maximum data variance. The first of the PCs is the one with the highest variance, which decrease for the next PCs. The algorithm followed by the PCA is:

- Input: $X \in R^{nxd}$; Output: $Y \in R^{nxk}$;
  1. Build the covariance matrix XX^T;
  2. Obtain Eigen values and Eigen vectors by applying Eigen decomposition to XX^T;
  3. Sort Eigen values from the higher to the lower;
  4. Build the *dxk* transformation matrix W with k top Eigen vectors;
  5. Uses W to transform X to obtaining the new subspace $Y = XW$.

The PCA algorithm uses a transformation matrix W with which it maps the original d-dimensional space X to a new k-dimensional space Y, with $k \leq d$ code. The PCs are the eigen vectors of the covariance matrix XX^T, obtained together with the eigen vectors by applying the linear eigen decomposition method to the covariance matrix. Eigen vectors and eigen values show the data direction and the data magnitude, respectively. Each column of the matrix W represents a different eigen vector, and they are ordered from the one with the highest associated eigen value to that with the lowest. The PCA technique is suitable for linear problems, but it does not operate well when used for non-linear data. In this case, the Kernel Principal Component Analysis, which represents a version of PCA suitable for non-linear scenarios, is a better candidate. PCA is used in [113] to conduct a data reduction process to lower the dimensionality of a dataset used for aircraft engine diagnostics. The dimensionality reduction capabilities of PCA are also employed in [114] with the goal of predicting the Remaining Useful Life (RUL) of airplane engines.

3.2.2. KPCA

The KPCA is a non-linear adaptation of the common PCA. KPCA operates by mapping the X matrix to a higher feature space $\phi(X)$ using polar coordinates. This projection is made by using the kernel method:

$$K(x_a, x_b) = \phi(x_a)^T \phi(x_b) \tag{3}$$

The kernel function avoids the mapping process with the function ϕ, which makes the process cheaper. The most common kernels exploited in KPCA are reported in Table 5.

Table 5. Commonly used kernels in KPCA.

Kernel	Description
Linear: $k(x_a, x_b) = {x_a}^T x_b + constant$	Generally used when data are linearly separable.
Polynomial: $k(x_a, x_b) = \left(\alpha {x_a}^T x_b + constant\right)^{degree}$	Shows the similarity among data in a feature space over the polynomials of actual variables.
Gaussian: $k(x_a, x_b) = \exp(-\frac{\lvert x_a - x_b \rvert^2}{2\sigma^2})$	Used when data are non-linearly separable.
Sigmoid: $k(x_a, x_b) = \tanh\left({x_a}^T x_b + constant\right)$	Mostly used in neural networks.

KPCA first applies the kernel method and subsequently uses the common PCA algorithm on the new linearly separable data. The algorithm followed is:

- Input: $X \in R^{nxd}$; Output: $Y \in R^{nxk}$;
  1. Produce linear data X' with kernel mapping function K to X;
  2. Uses the common PCA to X', obtaining reduced space Y.

KPCA is employed in [115] as a dimensionality reduction technique for datasets used in aircraft engine diagnostics. In [116], the data reduction capabilities of the KPCA are used to develop a method used for face recognition purposes. Another example of the application of the KPCA as an element to perform a data reduction process in a diagnostic tool used for aircraft engines is available in [117].

3.2.3. LDA

Linear Discriminant Analysis (LDA) is another technique used for FE, which works by identifying a new feature space by projecting data with the goal of maximizing the classes' separability. Starting from the d independent features of a dataset, the LDA extracts k new independent features that separate the dependent features the most, producing a number of components smaller than the number of classes—1. The algorithm followed is:

- Input: $X \in R^{nxd}$; Output: $Y \in R^{nxk}$;
  1. Obtain two scatter matrices of X: in-between-class and within-class;
  2. Calculate the eigen values and eigen vectors of the scatter matrices;
  3. Rank eigen vectors in descending order, based on eigen values;
  4. Build the transformation dxk matrix W with k top eigen vectors;
  5. Uses W to transform X to obtaining the new subspace $Y = XW$.

  The two scatter matrices are built with:

$$SM_b = \sum_{k=1}^{m} N_k(\mu_k - \mu)(\mu_k - \mu)^T \tag{4}$$

$$SM_w = \sum_{k=1}^{m} \sum_{x=1}^{n} (x - \mu'_k)(x - \mu'_k)^T \tag{5}$$

where SM_b and SM_w are the in-between-class and the within-class matrices, respectively, which compute the distance between the mean of each class and the distance between the mean of each class together with the data within the class. Furthermore, in Equations (4) and (5),

m represents the number of classes, μ denotes the overall mean, μ_k and N_k are the mean and sizes of the respective classes, respectively, and finally, μ'_k is the mean vector of a class. The final part of the algorithm represents the final part of the PCA algorithm. The LDA algorithm is used in [118] for FE purposes to develop a diagnostic tool for rolling bearings.

3.2.4. MDS

The Multi-Dimensional Scaling (MDS) method performs an FE process by focusing on the relationships between data in multi-dimensional space. Two main versions of the MDS algorithm exist: the metric MDS (or classic) and the non-metric MDS. The type here reported is the classic one. The algorithm followed by the classic MDS is:

- Input: $X \in R^{nxd}$; Output: $Y \in R^{nxk}$;
  1. Obtain the dissimilarity matrix d^X X;
  2. Compute K by utilizing the centering matrix H;
  3. Uses eigen decomposition with K to have top k Eigen values and corresponding vectors;
  4. Provide Y using diagonal matrix K and top k Eigen vectors.

MDS computes the dissimilarity matrix such that similar data are near and less similar ones are far apart. Starting from dissimilarity matrix d^X, MDS search the output Y for which the similarity between d^X and d^Y is maximized, where $d^X = \sqrt{x_a - x_b}$ and $d^Y = \sqrt{y_a - y_b}$ represent the distance between any two points a and b. The kernel matrix K is obtained with the following equation:

$$K = Hd^X H \tag{6}$$

in which the centering matrix is $H = I - \frac{1}{n}(ee^T)$, where I is the identity matrix and e is a column vector of 1 s. Applying eigen decomposition to K, the matrices D and B containing its eigen values and eigen vectors are obtained. After the selection of the top k eigen values, removing the rest of the eigen values and corresponding eigen vectors, matrices D and B become $\hat{D} \in R^{kxk}$ and $B_1 \in R^{nxk}$, representing the diagonal matrix of top k eigen values and the matrix containing the top k eigen vectors, respectively. Finally, the following equation:

$$Y = \hat{D}^{1/2} B_1^T \tag{7}$$

performs the mapping of the data to a low dimension. MDS is used in [119], located in a health monitoring system developed to monitor the health status of the landing gear retraction/extension system.

3.2.5. SVD

Singular Value Decomposition (SVD) is able to provide a representation of a dataset as a matrix with any number of dimensions. The precision of the representation of the SVD depends on the number of dimensions (components) chosen; the greater they are, the better the representation. In SVD, the following law is used to choose the top k largest singular values:

$$X = NSZ^T \tag{8}$$

where X is the original matrix; N is an nxk matrix of orthogonal unit vector columns, ordered by importance; S is a kxk diagonal matrix; and Z is a kxd orthogonal matrix. The SVD uses the following equation:

$$Y = N_k S_k Z_k^T \tag{9}$$

to obtain a reduced matrix Y in which only the top k singular values are retained. In Equation (9), N_k, S_k, and Z_k^T are a truncation of N, S, and Z^T. The diagonal entries of S are called the singular values. They are positive and arranged in descending order. The algorithm followed by SVD is:

- Input: $X \in R^{nxd}$; Output: $Y \in R^{nxk}$;
  1. Decompose X into matrices N, S and Z;
  2. Obtain Y by selecting k top singular values from S.

SVD is used in [120] together with PCA as a data reduction tool, which represents part of a more complex system developed to perform RUL estimation in aircraft engines.

3.2.6. LLE

Locally Linear Embedding (LLE) assumes that initial data lie on a smooth nonlinear manifold embedded in a high feature space to produce low-dimensional global coordinates. During feature reduction, LLE preserves the local properties of a data point x_a by means of the linear combination of the reconstruction matrix W_{ab} with the c-nearest neighbors x_b. LLE uses the Euclidean distance to find the c-nearest neighbors of each data. Subsequently, by reducing the reconstruction error (Equation (10)), the local weights for each data point (X_a), which are an optimal representation of the data (X'_a) as a linear combination of the neighbors, are calculated. Next, the Eigen vector-based optimization is used to obtain a new vector space Y. The weights with which the vectors (data points) are rebuilt from their nearest neighbors are computed. The reconstruction error is:

$$Err(W) = \sum_a \left| \vec{x}_a - \sum_b W_{ab} \vec{x}_b \right|^2 \tag{10}$$

which is minimized under the condition that all data (X_a) are rebuilt only from the nearest neighbors ($W_{ab} = 0$ when X_a and X_b are not neighbors) and that each row of the weight matrix gives a sum of 1, i.e., $\sum_b W_{ab} = 1$. The mapping of the data X_a from d-dimension to Y_a in k-dimension is obtained by minimizing the cost:

$$\phi(Y) = \sum_a \left| \vec{y}_a - \sum_b W_{ab} \vec{y}_b \right|^2 \tag{11}$$

The algorithm performed by the LLE is the following:

- Input: $X \in R^{nxd}$; Output: $Y \in R^{nxk}$;
  1. Find the c-nearest neighbors for each data point of X;
  2. Calculate local weights W with which data are best reconstructed (X') from their neighbors;
  3. Use the weights from the previous step to map X' to Y on k-dimensions by minimizing the cost.

An example of the application of the LLE for health monitoring purposes is available in [121], where it is present as a part of a diagnostic approach applied to a case of a gearbox.

3.2.7. ISOMAP

Isometric Mapping (ISOMAP) is a method that overcomes the problem of classical scaling that they are not able to operate with the nonlinear structure in a manifold. The first step determines the geodesic distances to obtain a neighborhood graph of the data, in which data x_a and their nearest neighbors are connected. Next, the algorithm finds the shortest path for each pair of data in the graph to approximate the geodesic distance between them, obtaining a pairwise geodesic distance matrix d^G. Subsequently, the MDS method with kernel matrix is applied to d^G. Equation (6) is applied to the matrix d^G, and finally, ISOMAP finds the low-dimension embedding of a data point by applying Equation (7).

The algorithm followed is:

- Input: $X \in R^{nxd}$; Output: $Y \in R^{nxk}$;
  1. Obtain the neighborhood graph of X;
  2. Compute the matrix d^G of the geodesic distances;
  3. Use MDS method with d^G to obtain the new space Y.

A practical example of the application of ISOMAP is available in [122], where it is used as a nonlinear data reduction tool for a diagnostic system developed to detect faults in rotating machines.

3.2.8. LE

Laplacian Eigenmap (LE) operates similarly to the LLE, searching low-dimension data by maintaining the local properties of a manifold. Initially, LE creates a neighborhood graph G' in which the data x_a and the related nearest neighbors are linked to each other. A weighted edge connects all the x_a and x_b data in G', and the Gaussian kernel function is used where the weights follow this equation:

$$WE_{ab} = e^{\frac{-|x_a - x_b|^2}{2\sigma^2}} \tag{12}$$

where WE_{ab} is the weight of the connection between x_a and x_b, and σ is the variance of the Gaussian leading to an adjacency matrix (W). The dimensionality reduction is performed by minimizing a cost function:

$$\phi(Y) = \sum_{ab} |y_a - y_b|^2 WE_{ab} \tag{13}$$

The cost function above can be reformulated as the Eigen decomposition problem:

$$\sum_{ab} |y_a - y_b|^2 WE_{ab} = 2YLY^T \tag{14}$$

where $L = W - D$ is the Laplacian matrix of G', D is a diagonal matrix whose elements are the row sums of W, and the W is a matrix with entries equal to 1 or 0 and with the diagonal entries equal to 0. The W entries suggests if a pair of vertices are adjacent or not. The FE technique is based on the following algorithm:

- Input: $X \in R^{nxd}$; Output: $Y \in R^{nxk}$;
  1. Construct the neighborhood graph G' of X using adjacency matrix W;
  2. Compute the weights of the edges of G';
  3. Optimize the cost function to obtain the new space Y.

LE is applied in [123], where a tool is developed to perform fault diagnosis and prognosis on turbofan engines.

3.2.9. ICA

Independent Component Analysis (ICA) is a linear and supervised technique. ICA can reduce the higher and second order dependencies of a dataset to create new features that are statistically independent. The ICA technique looks for directions that are independent from each other. ICA performs a decomposition of the matrix X:

$$X = AS \tag{15}$$

where A is the mixing matrix, while S is the independent components. Subsequently, create the Y matrix by selecting the top k independent components:

$$Y = A_k S_k \tag{16}$$

The algorithm of the ICA follows these steps:

- Input: $X \in R^{nxd}$; Output: $Y \in R^{nxk}$;
  1. Performs a decomposition of X to A and S;
  2. Select top k independent components;
  3. Obtain Y exploiting the k components.

The ICA is used in [124], where a technique able to detect the presence of debris in the exhaust gases of aircraft engines by means of electrostatic induction is presented. Another example of the application of the ICA is available in [125], where an intelligent system to detect and diagnose induction motor faults is developed.

3.2.10. t-SNE

t-Distributed Stochastic Neighbor Embedding (t-SNE) is a nonlinear, unsupervised, and manifold-based reduction method in which data mapping from a higher to a low dimension takes place by preserving the significant structure of the original data. T-SNE performs a conversation of the high-dimensional Euclidean distances into conditional probabilities representing similarities for every pair of data. The equation:

$$P_{a|b} = \frac{e^{\frac{-\|x_b - x_a\|^2}{2\sigma^2}}}{\sum_{a \neq k} \frac{-\|x_k - x_a\|^2}{2\sigma^2}} \quad (17)$$

where $P_{a|b}$ is the conditional probability which represents the similarity of data x_a to data x_b and provides information about the proximity of the two data points x_a and x_b, considering a Gaussian distribution around x_b with a variance σ^2. Subsequently, the set of probability $Q_{a|b}$ in the low-dimensional space is computed by means of a Student's t-distribution with one degree of freedom. Finally, the method minimizes the difference between the two cited probabilities from the low-dimensional to the high-dimensional spaces. The difference is given by the optimization of the cost function ϕ:

$$\phi = \sum_a \sum_b P_{a|b} log \frac{P_{a|b}}{Q_{a|b}} \quad (18)$$

The steps of the t-SNE algorithm are:

- Input: $X \in R^{nxd}$; Output: $Y \in R^{nxk}$;
  1. Compute the conditional probabilities $P_{a|b}$ and $Q_{a|b}$;
  2. Minimize the difference between $P_{a|b}$ and $Q_{a|b}$ to perform a mapping process of X to Y.

The properties of the t-SNE algorithm are exploited in [126,127] in the development of an engine fault diagnosis tool.

3.2.11. Summary of Data Reduction Methods

Table 6, which is built with information available in the tables present in [111,112], summarizes the data reduction techniques reported together with our addition of some Refs, in which their application for health monitoring purposes is shown.

Table 6. Collection of the data reduction methods listed in this paper and taken from [112].

Method	Supervision	Coupled with	Advantages	Disadvantages	In EHM
PCA	Unsupervised	ANN * [113,114].	Eliminates the correlation between the features. Improves data visualization.	Not adaptive to nonlinear cases. Do not work in cases in which mean and covariance do not completely define the dataset.	[113,114]
LDA	Supervised	TET *.	Data are classified into groups.	Suffers from a class singularity issue.	[118]
MDS	Unsupervised	FCM *.	Preserves the distances in cases in which it is difficult to represent a low number of dimensions [128].	Needs a lot of computation and memory.	[119]
KPCA	Unsupervised	ANN [115,117].	More suitable in nonlinear cases.	Long training time.	[115,117]
SVD	Unsupervised	ANN.	Works efficiently with sparse matrices.	Not adaptive to nonlinear cases.	[120]

Table 6. *Cont.*

Method	Supervision	Coupled with	Advantages	Disadvantages	In EHM
LLE	Unsupervised	KSR *.	Fast and capable of preserving local geometry.	Requires more memory and less efficient with noised data.	[121]
ISOMAP	Unsupervised	Not specified classifier.	Relationship between data points is preserved.	Suffers from topological instability.	[122]
LE	Unsupervised	SVM * for diagnostics and PHM * for prognostics.	Gives a unique solution.	May produce disconnected neighborhood graph.	[123]
ICA	Supervised	Used as denoiser in electrostatic monitoring [124]; SVM [125].	Is able to filter noise from the signal.	Long training time.	[124,125]
t-SNE	Unsupervised	No diagnostic or prognostic algorithms. Based on spatial structural characteristics of QAR * data [126]; ANN [127].	Works efficiently with nonlinear data.	Provides only 2 or 3 features. Computationally complex.	[126,127]

* ANN: Artificial Neural Network; TET: Transient-extracting Transform; FCM: Fuzzy c-means; KSR: Kernel Sparse Representation; SVM: Support Vector Machine; PHM: Cox proportional hazards model; QAR: Quick Access Recorder.

4. Diagnostic and Prognostic Techniques

As previously discussed, CBM is a maintenance-optimization strategy utilized in the aviation industry to achieve cost savings, improve flight safety, and streamline maintenance management [129]. The principal disciplines constituting CBM are diagnostics and prognostics [26]. Diagnostics is the field that deals with assessing the condition of a system based on information provided by its intrinsic physical parameters. In the context of aircraft engines, diagnostics refers to the process of determining the condition of the engine and/or its components using data from sensors or information gathered from visual inspections [26]. Prognostics, on the other hand, is the field that deals with forecasting the remaining lifespan of a system, based on historical and current data related to the system's condition. In the aviation industry, prognostics is widely used to estimate the RUL of engines by analyzing data from previous flights and in-flight data obtained from sensors [130].

Figure 10 presents an illustration of diagnostic and prognostic approaches. These methods can be divided into two main categories: model-based methods and data-driven methods. Model-based methods are based on a mathematical model of the engine, which links the non-measurable and measurable parameters of the engine with mathematical and thermodynamic equations that describe the engine's behavior and from which the degradation process can be predicted. On the other hand, data-driven methods do not rely on mathematical models of the engine, which can be difficult to obtain due to a lack of information about the gas turbine parameters and component maps. Instead, they are based on a set of historical data on gas turbine measurements under various operating conditions, from which they can identify trends. In recent years, research has also focused on developing hybrid methods [26,32,131,132]. In the present section, a list of the most used diagnostic and prognostics technique is presented and explained [25,39,133–135].

4.1. Model-Based Methods

4.1.1. Gas Path Analysis (GPA)

The objective of the GPA is to detect the occurrence of a fault in a component by monitoring certain parameters related to its condition [136,137]. As reported in [32], GPA was introduced by Urban [138] and later made more popular in the 1980s thanks to Saravanamuttoo et al. [139,140].

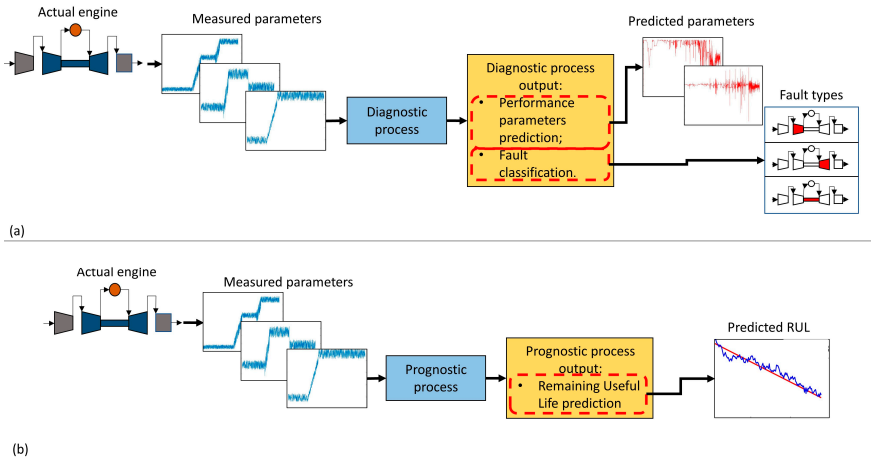

Figure 10. Diagnostic and prognostic processes illustration. (**a**) Overview of a diagnostic process; (**b**) Overview of a prognostic process.

The goal of detecting, isolating, and quantifying certain faults can be achieved if the fault in question results in a change in the measurable (i.e., dependent) variables [141]. Independent variables, such as flow capacity and efficiencies, which can serve as a health indicator for the components, are not directly measurable, but are physically linked to the measurable (or dependent) variables, such as temperatures or pressures. Therefore, a change in independent variables (not measurable) results in a change in dependent (measurable) variables. In an arbitrary GT configuration, dependent variables Z are expressed as a function, such as:

$$Z = F(I, H) \tag{19}$$

where I denotes the input vector, i.e., the operating conditions; the functions of ambient temperature and pressure, and of power-setting parameters. Meanwhile, H is the independent variables vector containing the PPs of the components such as flow capacities and efficiencies [141]. Considering a very small change in health parameters and a fixed operating point, a linear approximation can be performed:

$$\delta Z = ICM \cdot \delta H \tag{20}$$

This is the equation for Linear GPA, ignoring measurement noise and bias. ICM stands for Influence Coefficient Matrix, which can be obtained by solving a set of differential equations expressing the thermodynamic relationship between dependent and independent variables, or with an approximate approach that involves perturbing the independent variables one at a time and observing their effect on the dependent variables [141]. Inverting the ICM, the Fault Coefficient Matrix (FCM) is obtained, and changes in independent variables are obtainable by the change in dependent ones as:

$$\delta H = FCM \cdot \delta Z \tag{21}$$

However, a linear approximation is suitable for a fixed operating condition and assuming little change in dependent and independent variables. When large variations in operating conditions and severe degradation are taken into account, Linear Gas Path Analysis (LGPA) becomes less reliable. These limitations can be overcome by introducing Non-Linear Gas Path Analysis (NLGPA), which can be obtained through successive iterations using LGPA and the Newton–Raphson method until an exact solution of the non-linear equation 19 is obtained [137]. As mentioned in [137], each independent parameter can be expressed individually as a unique function of the dependent parameters. Denoting with:

$$F(H) = Z \tag{22}$$

the relation between dependent and independent variables and considering a small change in H:

$$F(H + \delta H) = Z + \delta Z \tag{23}$$

which becomes:

$$F(H + \delta H) = F(H) + \delta Z \tag{24}$$

Using Taylor series expansion, the term $f(H + \delta H)$ can be rewritten as:

$$F(H + \delta H) = F(H) + J \cdot \delta H + HOTs \tag{25}$$

Jacobian notation is used to refer to the first derivative of the matrix function $F(H + \delta H)$ in the Taylor Series, that is:

$$J = \begin{bmatrix} \frac{\partial f_1(H)}{\partial h_1} & \frac{\partial f_1(H)}{\partial h_2} & \cdots & \frac{\partial f_1(H)}{\partial h_m} \\ \frac{\partial f_2(H)}{\partial h_1} & \frac{\partial f_2(H)}{\partial h_2} & \cdots & \frac{\partial f_2(H)}{\partial h_m} \\ \vdots & \vdots & \ddots & \vdots \\ \frac{\partial f_n(H)}{\partial h_1} & \frac{\partial f_n(H)}{\partial h_2} & \cdots & \frac{\partial f_n(H)}{\partial h_m} \end{bmatrix} \tag{26}$$

and:

$$\delta H = [\partial h_1 \partial h_2 \vdots \partial h_m] \tag{27}$$

where h_i with $i = 1, 2, \ldots, m$ are the independent parameters and f_j with $j = 1, 2, \ldots, n$ are the relations between dependent and independent parameters. For small variation in H, $HOTs$ can be neglected and Equation (25) becomes:

$$F(H + \delta H) = F(H) + J \cdot \delta H \tag{28}$$

Combining Equations (24) and (28):

$$\delta Z = J \cdot \delta H \tag{29}$$

By inverting J, as described by Donaghy [142]:

$$J^{-1} \cdot \delta Z = \delta H \tag{30}$$

the correction δH to the independent variable is added to the solution vector:

$$H_{new} = H_{old} + \delta H \tag{31}$$

The iterative process is repeated until a state of convergence is achieved. More exhaustive information is available in [137]. In [143] are presented some examples on GPA application for different purposes, such as component condition monitoring, the analysis and validation of essential performance parameters used for EHM, and the prediction of the effect of component performance restoration. The results demonstrate a good diagnostic performance and the utility of performing a performance restoration effect analysis. Zhou et al. [144] proposed a fault diagnosis and prognosis method based on a long short-term memory neural network and GPA algorithms. More specifically, in the work, the health parameters diagnosed by means of GPA are used to predict the future degradation of components. The results show that the Root Mean Squared Error (RMSE) of the diagnosed health parameters remains below 0.193%, and equals 0.232%, 0.029%, 0.069%, and 0.043% for the predicted health parameters of each component, considering the best prediction model tested. Figure 11, adapted from [39], shows an illustration useful to compare LGPA and NLGPA approaches.

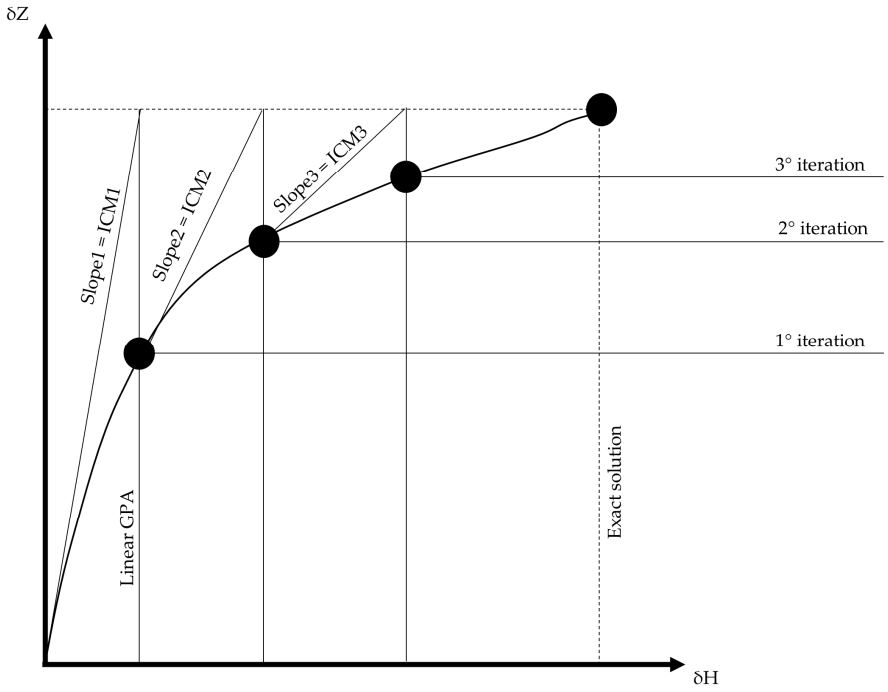

Figure 11. Iterative process of the NLGPA algorithms [39].

4.1.2. Kalman Filters (KFs)

KFs were presented by Kalman in 1960 [145]. KFs are a specific type of Bayesian recursive filter and are particularly well-suited for state estimation in cases of linear systems and Gaussian noise [146]. Kalman Filters (KFs) are widely used in applications such as satellites, spacecrafts, and aircrafts for the purpose of automatic control of the systems [147]. KFs are a widely used technique in aircraft engine diagnostics. In [148], a comparison of the capabilities of KFs and neural networks to isolate a single GT fault is presented. The results demonstrate a comparable level of accuracy between the methods, with slightly better performance from the KF approach. In [149–151], Kobayashi and Simon investigate the capabilities of KFs for sensor and actuator fault detection and isolation, as well as the detection of component faults. The accuracy of the developed system is evaluated through a series of simulations of various engine faults. A similar research is proposed in [152]. For interested readers, other examples are available in [153–155]. KFs utilize a recursive solution, meaning each updated estimate of the state is calculated from the previous estimate and the new input data [156]. According to Luppold et al., Kalman Filters (KFs) are a data processing algorithm utilized to estimate both system states and unmeasurable parameters in real time [157]. KFs are suitable for linear systems. Adaptations for non-linear systems include Extended KFs (EKFs) and Unscented KFs (UKFs). A more detailed explanation of KFs, EKFs, and UKFs can be found in [158]. In [159], KFs are used to develop a tool for prognosis purposes with multiple sources of uncertainty. The method has been tested on an aircraft fuel feeding system case and has shown good results. Figure 12 illustrates the engine health monitoring approach using KFs [160].

4.1.3. Genetic Algorithms (GAs)

Developed by John Holland at the University of Michigan, GAs are algorithms that take inspiration from the mechanism of natural selection, where the “fittest” individuals pass on their characteristics to the next generation [161].

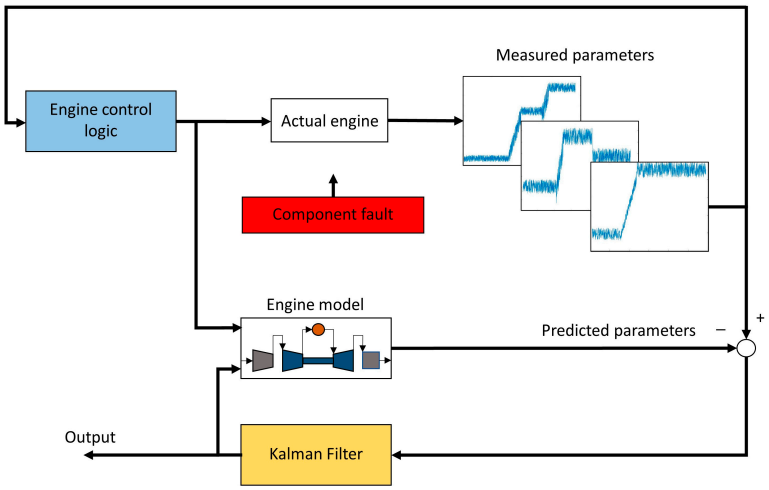

Figure 12. GT health monitoring using KFs.

In a GA, a set of solutions (referred to as "individuals") for a specific problem is initially generated randomly. This set of solutions is referred to as the "population", and each of them represents the current iteration's generation. The fitness of each candidate solution is determined by evaluating an objective function of the optimization process that needs to be solved. The more fit solutions are selected and used to form the next generation. The solutions in this new generation are subject to the same process as their "parents". The iterative process continues until a stopping criterion is met, such as reaching a maximum number of generated generations or achieving a target level of fitness [26,162–164]. Each iteration of a GA comprises three main steps: selection, crossover, and mutation. In the selection phase, individuals are chosen for the next generation based on their level of fitness. In the crossover phase, information is exchanged between different individuals to create fitter individuals. Finally, in the mutation phase, certain existing individuals are randomly altered within predetermined upper and lower thresholds to create new individuals [165]. More exhaustive treatises on GAs are available in [166,167]. GAs are exploited in [168] to detect and estimate sensor bias, in order to enhance the estimation of health parameters using a neural network. In [169], a diagnostic tool based on GAs is used for a turbofan engine to detect power-setting sensor faults, also in combination with engine component degradation and sensor faults. An interesting application of GAs is reported in [170], where they were used for the optimization of neural network topology. Similarly, GAs are used in [171] to optimize the parameters of decision tree-based methods for RUL prediction. Figure 13, adapted from [39], illustrates an example of a GA reproduction cycle.

4.2. Data-Driven Methods

4.2.1. Artificial Neural Networks (ANNs)

ANNs are algorithms designed to mimic the behavior of the human nervous system, enabling them to learn from experience [172]. These algorithms can find a correlation between two sets of variables, the input and the output, and use this learned correlation to predict a new set of output variables based on a new set of input variables. Artificial neural networks (ANNs) consist of layers and neurons. The first and last layers are known as the input and output layers, respectively. Each layer is composed of a certain number of neurons. The input and output layers contain several neurons equal to the number of input and output variables, respectively. The layers located between the input and output layers are known as hidden layers, and they contain hidden neurons. The performance of the network depends on the number of hidden layers and neurons, which can be challenging to determine [173].

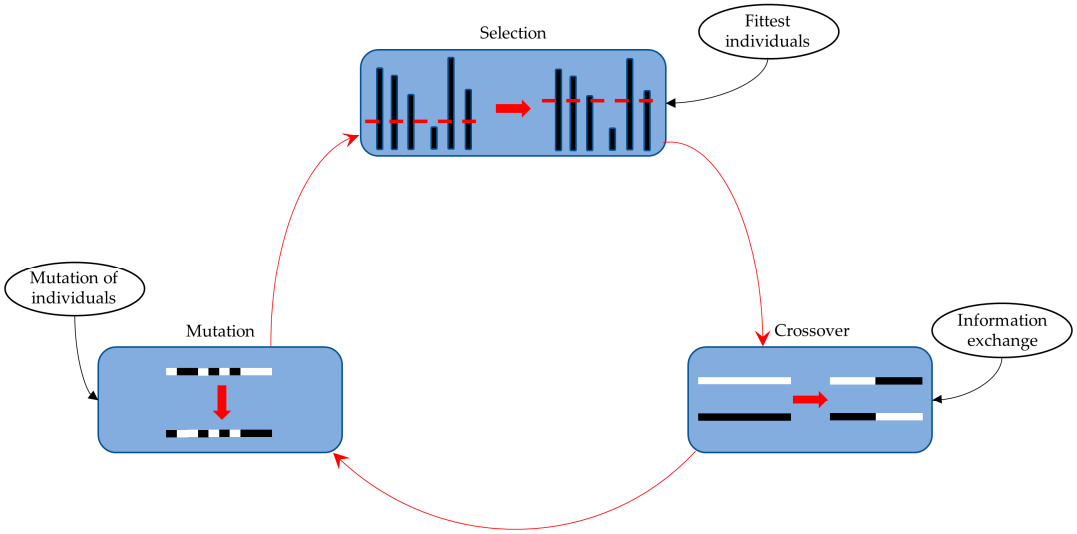

Figure 13. Reproduction cycle of a GA [39].

Each neuron in the hidden and output layers is connected to the neurons in the preceding layer and each connection has a weight. The purpose of these neurons is to process information received from the preceding neurons, and in turn, provide information that is dependent on the input, as described by the following equation:

$$O = \sum_{i=1}^{l} W_i INF_i + b \tag{32}$$

where l represents the number of previous neurons from which information is received, O represents the neuron output, W_i represents the connection weight with the i-th previous neuron, INF_i represents the information deriving from the i-th previous neuron, and b represents an added bias. The output of a neuron is limited by an activation function. There are many types of neural networks today, which can be broadly divided into two main categories: Feed-Forward Neural Networks (FFNNs) [174] and Recurrent Neural Networks (RNN) [175–177]. FFNNs are simple networks composed of layers and neurons, as previously described. If each neuron in each layer has a connection with every neuron in the next layer, the FFNN is referred to as fully connected. On the other hand, if some connections are missing, the FFNN is referred to as partially connected. Recurrent neural networks (RNNs) are designed to learn sequential or time-varying patterns [176] and differ from FFNNs due to the presence of at least one feedback loop. This feature provides a great deal of flexibility and allows RNNs to approximate arbitrary dynamic systems with high precision. A single-loop feedback network is a type of RNN that has a single feedback loop [172,175]. Figure 14 illustrates the difference between the typical structures of a FFNN (7.a) and a RNN (7.b). ANNs were used in [178] for the purpose of predicting performance and engine health status. The results obtained from applying the ANN-based diagnostic tool on a single spool turbojet experiencing compressor and turbine degradation were compared to the results obtained from another diagnostic technique that used a support vector machine (SVM) developed in the same study. Both the ANN and SVM techniques yielded very good and comparable results in predicting the EGT and fuel flow during a specific flight, with an RMSE ranging between 0.0089 and 0.0191. However, when used for engine health prediction, the SVM technique performed extremely well, while the ANN technique showed a less efficient performance. In [179], ANNs form the basis of a prognostic method.

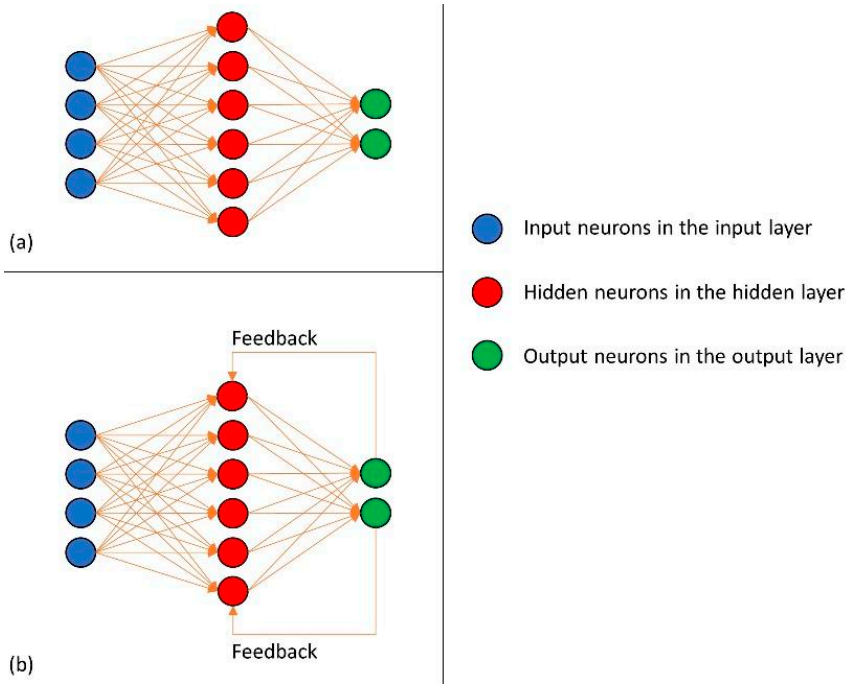

Figure 14. (**a**) Typical structure of FFNNs; (**b**) typical structure of RNN.

The study focused on predicting the remaining useful life (RUL) of a fan module. ANNs were used to estimate current health parameters, such as efficiency and flow capacity, and the future trajectory of these parameters was estimated using an autoregressive model. RUL estimation was performed based on the estimated trajectory of the health parameters using moving window and progressive window approaches, which differ in how data are fed to the autoregressive model. It was found that the progressive window approach yielded the best results.

4.2.2. Bayesian Belief Networks (BBNs)

A belief network is a graphical representation of a probability distribution that depicts the cause-and-effect relationships among predisposing factors, faults, and symptoms [180]. The graph represents a set of variables indicated by nodes and directed edges indicating their dependencies. The level of relationship between variables is represented by a conditional probability [39,181]. In a BBN graph, three types of nodes can be distinguished: child nodes, which are nodes with edges directed towards them; parent nodes, which are nodes from which edges originate; and root nodes, which are nodes without any edges directed towards them. In an aircraft engine diagnostic approach, by setting independent variables such as flow capacities and efficiencies as parent nodes, and dependent variables such as temperatures, pressures, etc., as child nodes, the BBN approach expresses the diagnostic problem as:

$$P(h_i/z_j) = \frac{P(z_j/h_i)P(h_i)}{P(z_j)} \tag{33}$$

where h_i and z_j are the i-th independent and j-th dependent variables, respectively; $P(h_i/z_j)$ is the probability of h_i given z_j; $P(z_j/h_i)$ is the probability of z_j given h_i; $P(h_i)$ is the probability of the independent parameter h_i; and $P(z_j)$ is the probability of the dependent parameter z_j [39]. Figure 15, adapted from [39], shows an example of a BBN structure used for GT diagnostic purposes.

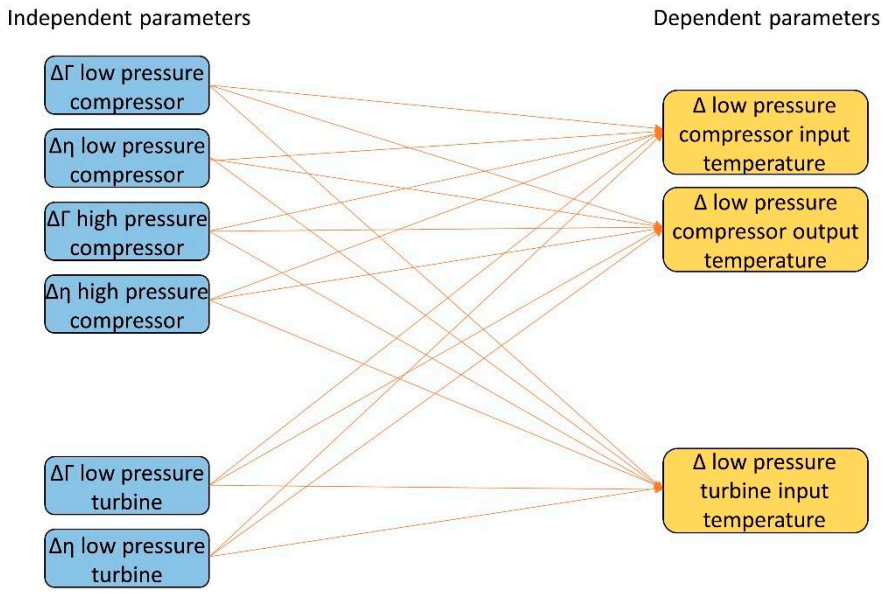

Figure 15. Typical BBN structure for GT diagnostic purposes. Adapted from [39].

BBNs were first applied for gas turbine diagnostics in the 1990s by Breese et al. [182]. In [183], a BBN that includes 11 health parameters and seven measured parameters is used to develop a diagnostic tool for detecting faults in a turbofan engine. The BBN considers deviation in flow parameters and efficiencies as potential indicators of faults. Mast et al. [184] applied a series of Bayesian Belief Networks (BBNs) for diagnostic purposes for a turbofan engine and conducted tests under different flight conditions. They found that fault detection is easier during cruise phases compared to take-off and climb phases. Ferreiro et al. [185] employed Bayesian Belief Networks (BBN) as a means to develop a prognostic technique for predicting brake wear on an aircraft. The paper describes the use of two different BBN-based models.

4.2.3. Expert Systems (ESs)

ES are computer programs designed to mimic the decision-making processes of an expert human in solving problems or providing advice [164]. The typical components of an ES are: a user, a developer, an inference engine, and a knowledge base. The knowledge base stores the information necessary to solve a specific problem, and it serves as the substitute for the human expert. The inference engine acts as a bridge of communication between the user and the "virtual expert" (the knowledge base) by linking the user's queries with the relevant answers stored in the knowledge base. This task is performed by utilizing appropriate programmed rules to establish a relationship between multiple items. Finally, the developer designs the expert system and supplies the necessary knowledge [186]. Basic ES utilize Boolean logic or decision trees, which can present limitations in accurately representing real-life problems due to their simplicity. More advanced ES employ inference rules and chaining, which are programmed as IF-THEN statements [39]. Figure 16, adapted from [39], shows a classical structure of an ES. ES have been utilized to create a variety of diagnostic systems for different types of engines [39,135], such as TEXMAS (Turbine Engine Expert Maintenance Advisor System) for T53 engines [187]; HELIX (HELicopter Integrated eXpert) [188] for helicopter engines; XMAN, a tool for automated jet engine diagnostics [189]; TIGER (Testability Insertion Guidance Expert System) [190]; IFDIS (Interactive Fault Diagnosis and Isolation System); and SHERLOCK, for helicopter engines.

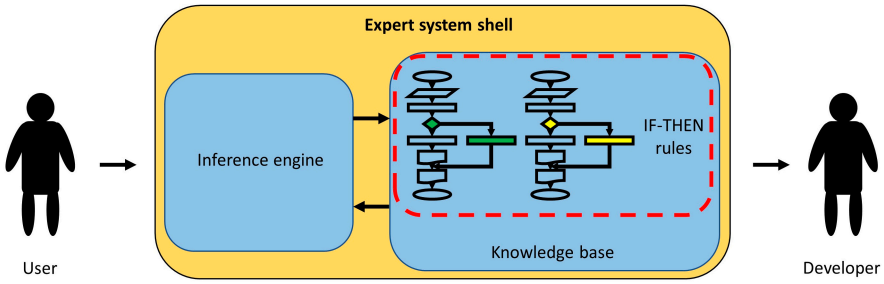

Figure 16. Generic structure of an ES. Adapted from [39].

4.2.4. Fuzzy Logic (FL)

Introduced by L. Zedah in the 1960s [191,192], fuzzy sets, which are sets formed by elements that have degrees of membership, were thought to mathematically model the uncertainty of natural language [193]. Fuzzy logic (FL), which is based on fuzzy sets, is used to simplify complex phenomena. The quality of the simplification is dependent on the availability and quality of the rules used [194]. A general FL system comprises several essential components, including fuzzy rules, a fuzzifier, inference engine, and a defuzzifier. The fuzzifier is responsible for the process of fuzzification, where input signals are converted into fuzzy sets. The inference engine establishes the relationships between the various fuzzy sets. The defuzzifier performs the process of defuzzification, resulting in the output signals. Finally, the fuzzy rules represent a collection of IF-THEN statements utilized to implement FL [39,135]. Figure 17, adapted from [194], shows a typical FL system structure.

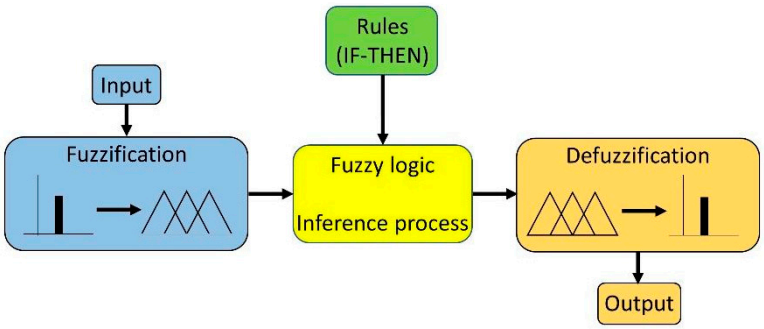

Figure 17. The typical structure of an FL system.

FL has been extensively employed for fault diagnosis in aircraft engines. In [195], a FL system is implemented for diagnostic purposes on a military turbofan engine. In this case study, the FL system developed predicts the condition of the intermediate pressure compressor with an average error of approximately 7.5%. Another application of FLs for fault identification is shown by Ganguli [196,197], which utilizes FLs to develop a fault isolation system for a turbofan engine. The system is able to recognize faults in the fan, low-pressure compressor, high-pressure compressor, high-pressure turbine, and low-pressure turbine based on deviation from the baseline (when the engine is in a healthy condition) of certain parameters, such as exhaust gas temperature, fuel flow, and low and high rotor speed. Similarly, in [198], a case study of a three-spool engine is analyzed. Fuzzy Logic (FL) is used to create single fault isolation and partial multiple fault isolation systems (with only two components considered faulty). Sensor noise and biases are added, and the results demonstrate excellent performance in each case studied. In [199], FL is used for the same purposes. The developed system is tested using flight data, and the results show the detection of a fault in the high-pressure spool two months before it occurred.

4.2.5. Support Vector Machine (SVM)

SVMs are a type of learning system based on statistical learning theory, and they are commonly used for classification or regression tasks [32,200]. Like ANNs, SVM algorithms require a set of inputs (or features) and a corresponding set of outputs for the training phase. Each input can be thought of as a dimension of a hyperplane. The goal of SVM is to create a hyperplane that separates the input space into two or more classes, with the goal of achieving the maximum separation between the classes. By doing this, the expected generalization error is minimized, meaning the probability of incorrectly classifying new, unclassified features during the classification process is reduced. The process of maximizing separation is achieved by creating two parallel hyperplanes, known as the "bounding planes," on either side of the separating hyperplane. The distance between these bounding planes is called the "margin." The learning process of an SVM involves finding a hyperplane with the greatest margin and the least misclassification errors [201]. Figure 18 illustrates an example of the structure of SVMs used for fault classification [202]. In the aforementioned paper, SVMs were used in conjunction with Artificial Neural Networks (ANNs) to develop a diagnostic system that can effectively classify single, double, and triple component faults, and subsequently predict the magnitude of the faults with high accuracy.

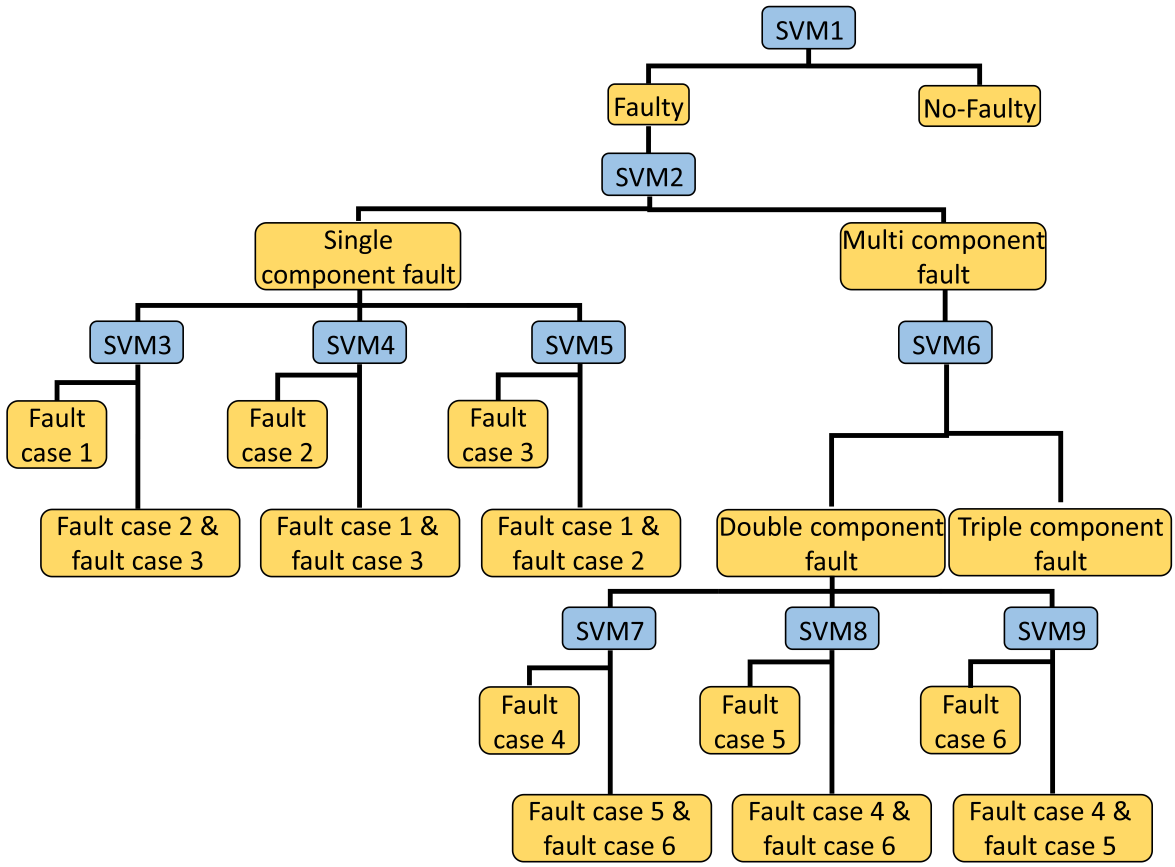

Figure 18. An example of the net of SVMs used for fault classification purposes.

During the training process of an SVM, a Kernel function and a set of parameters known as "Kernel parameters" must be selected. The performance of the SVM is highly dependent on the choice of these parameters [203]. In [200], the authors investigate the impact of various kernel functions (linear, polynomial, radial basis, and sigmoidal) and training sample size on the performance of an SVM for gas turbine fault diagnosis. They compare these results to those obtained using a neural network. Two samples of small size have been used. The results indicate that the sample size has a minimal effect on performance when using the radial basis kernel function, which shows the best results. However,

the effect of sample size on performance is more significant when using other kernel functions. Additionally, the study also examines the impact of including the compressor outlet temperature in the training dataset, considering different kernel functions and sample sizes. Finally, the performance of the SVMs trained with the four different kernel functions was compared to the performance of a neural network. The results showed that the SVM trained with the radial basis function performed better than the neural network for various sample sizes. Furthermore, increasing the sample size led to improved performance for all four of the tested kernel functions when compared to the neural network. SVMs are used in [204] to perform multi-class classification for fault diagnosis in a JT9D aero engine. Various approaches are compared to one another, and noise at different magnitudes is added to the data. As expected, the results show a decrease in accuracy with an increase in noise level. An example of the application of SVMs for prognostic purposes can be found in [205]. In this paper, the authors propose a method for classifying the health of an aircraft component, using a training dataset that includes flight data and maintenance logs. The method was applied to classify the health state of a bleed valve in the air management system as either healthy or unhealthy, in terms of a low or high probability of failure over a specific period of time.

4.3. Final Summary

As it is evident, numerous studies are focused on developing diagnostic and prognostic techniques to monitor the health status of aeronautical engines and other systems. Each study employes its own diagnostic or prognostic tool, developed using different techniques and approaches, and utilizing different types of data. In conclusion, Tables 7 and 8 present a comprehensive collection of some of the works available in the literature. For a more in-depth understanding, it is recommended to refer to the corresponding references.

Table 7. List of some works present in the literature with relative characteristics. For a more detailed description, read the corresponding references. Continues in Table 8.

Method	Type	Purposes	Machine	Data Type	Noise	Used Software	Refs.
KF	MB *	Diagnostics	Military twin-spool turbofan engine	Model data	Yes	-	[149]
KF	MB *	Prognostics	Aircraft fuel feed system	Model data	Yes	-	[159]
GA	MB *	Diagnostics	Aircraft two-shaft turbofan engine	Model data	No	Pythia	[169]
ANN/SVM	DD *	Performance analysis and diagnostics	Aircraft single-spool turbojet engine (Rolls Royce VIPER 632-43)	Measured and Model data	Yes	ONX and AEDSYS coupled MATLAB routines	[178]
ANN	DD *	Prognostics	Aircraft turbofan engine	Model data	-	ProDiMES for simulations; MATLAB for ANN implementation	[179]
BBN	DD *	Diagnostics	Aircraft turbofan engine	Measured and Model data	Yes	-	[183]
BBN	DD *	Diagnostics	Aircraft turbofan engine (GE CFM56-7)	Model data	-	MATLAB	[184]
BBN	DD *	Prognostics	Aircraft brake	Measured data	-	-	[185]
FL	DD *	Diagnostics	Military three-spool turbofan engine	Model data	Yes	Turbomatch for data generation; MATLAB for fuzzy logic implementation	[195]
FL	DD *	Diagnostics	Aircraft turbofan engine	Model data	Yes	-	[196]

* MB: Model-based; DD: Data-driven.

Table 8. List of some works present in the literature with relative characteristics. For a more detailed description, read the corresponding references. Continuation of Table 7.

Method	Pre-Processing	Metrics	Accuracy Based on Metrics on the Third Column	Type of Degradation	Refs.
KF	-	Minimum bias which can be isolated	0.8%	FOD, considering two different baselines, one healthy and one degraded, together with sensors and actuator faults	[149]
KF	Feature extraction and filtering	MSE	Between 0.000168 and 0.214	Cavitation erosion in booster pump	[159]
GA	-	Fitness (consult the paper for the definition)	Between 0.35 and 1	Power-setting sensor fault (with and without the presence of engine component degradation and other gas path sensor faults)	[169]
ANN/SVM	-	(a) Performance prediction: RMSE; (b) Diagnostics: prediction efficiency	(a) Between 0.019 and 0.0089; (b) Prediction efficiency between 80% and 100% in diagnostics	Compressor fouling and turbine erosion, one at a time and simultaneously	[178]
ANN	-	-	-	Fan abrupt fault	[179]
BBN	Filtering	Number of cases correctly diagnosed	13 out of 15 with measured data; About 90% during climb and cruise and about 60% during descent with model data	Different fault cases, including fault in FAN, LPC *, HPC *, HPT *, LPT * and nozzle	[183]
BBN	-	% of correct: (a) Identification; (b) Isolation	(a) Between 19.17% and 100%; (b) Between 7.33% and 86.79%	No degradation type is specified	[184]
BBN	-	Error between real and predicted brake wear	Between 4.0036 and 0.8012 in absolute value at last prediction	Brake wear	[185]
FL	-	Average percentage error between predicted and target	7.5%	IPC * fault	[195]
FL	-	% of correct fault isolation	Between 89% and 100%	FAN, LPC *, HPC *, HPT * and LPT * fault	[196]

* LPC: low-pressure compressor; HPC: high-pressure compressor; HPT: high-pressure turbine; LPT: low-pressure turbine; IPC: intermediate-pressure compressor.

5. Conclusions

Modern GTs are highly complex machines composed of a large number of components, each of which may be susceptible to various types of damage. As the number and complexity of parts increases, it leads to a higher probability of failure and a decrease in reliability. For GTs used in aircraft engines, reliability is of paramount importance. The reliability of a system is closely linked to the maintenance plan it is subject to. To enhance reliability and reduce maintenance costs, an effective maintenance plan is crucial, which can accurately predict the optimal time for performing maintenance. As a result, current research is focused on implementing CBM strategies, which schedule maintenance interventions based on the actual health status of the monitored system, rather than relying on traditional corrective and preventive maintenance strategies that are based on visual inspections and the probability of potential failures. This paper aimed to examine the primary degradation mechanisms to which gas turbines are typically subjected, highlighting the effect each of them has on the machine's performance. Subsequently, the paper presented the main techniques currently used for the implementation of the two key disciplines of CBM: diagnostics and prognostics. These techniques are based on the real-time health status of the monitored component, which is obtained through the use of appropriate sensors that provide useful information. Sensor measurements are then utilized to implement the algorithms for the developed diagnostic or prognostic technique. However, it should be noted that sensor measurements are not always free of noise and bias, which can negatively impact the performance of the techniques used to monitor the health status. A significant portion of research efforts are directed towards developing techniques for improving the quality of sensor measurements, in order to reduce the amount of noise present in the

sensed information, and to detect and isolate faulty sensors. In some cases, these techniques may also reconstruct the values lost due to incorrect detection by a damaged sensor. The performance of health monitoring techniques is dependent on the amount and accuracy of information collected from the monitored system. As the amount of data increases, so does the computational time and effort required. To improve performance, researchers are also developing techniques for data reduction. There are many types of computer algorithms currently used for diagnostic and prognostic purposes, each with their own advantages and limitations. Hybrid techniques, which combine multiple approaches, are an area of ongoing research, and future efforts are focused in this direction. In recent years, there has been growing scientific interest in the use of hybrid engines to reduce their environmental impact, which is an extremely important topic. However, most of the literature on degrading phenomena, data reduction techniques, and diagnostic and prognostic algorithms related to the aeronautical world has focused on thermal engines. Hybrid engines are composed of both thermal and electric components, and an increase in the number of components can lead to a decrease in reliability. Therefore, there is a need to study the application of CBM to hybrid engines, which represent the future of aviation and beyond. It is crucial to fully understand the degradation mechanisms of the electrical portion of a hybrid engine (i.e., related to components such as batteries, electric motors, dynamos, etc.) and their effect on engine performance to properly develop modern CBM systems suitable for hybrid engines.

Finally, regarding degradation health monitoring techniques, there are several gaps in the existing literature that require further exploration and research. These gaps include:

i. Lack of standardization: The field currently lacks standardized techniques and metrics for monitoring degradation, which can lead to inconsistencies across studies. Developing standardized techniques could help improve the reliability and consistency of results.
ii. Limited real-world testing: Most studies on degradation health monitoring techniques have been conducted in laboratory or simulated environments, which may not accurately represent real-world conditions. Further testing in real-world environments could provide more relevant and realistic data.
iii. Lack of comparative studies: While many studies have evaluated the performance of individual monitoring techniques, there is a lack of comparative studies that assess the strengths and weaknesses of different techniques for monitoring the same type of degradation.
iv. Insufficient consideration of uncertainty: Many monitoring techniques provide point estimates of degradation levels without accounting for the uncertainty associated with these estimates. Considering uncertainty could improve the reliability of degradation predictions.
v. Limited consideration of multiple degradations: Many studies focus on monitoring a single type of degradation, but real-world systems often experience multiple degradations simultaneously. Exploring how to monitor multiple degradations could provide a more comprehensive understanding of system health.

Author Contributions: Conceptualization, M.G.D.G. and A.F.; methodology, M.G.D.G.; software, N.M.; investigation, N.M.; resources, A.F.; writing—original draft preparation, N.M. and M.G.D.G.; writing—review and editing, M.G.D.G.; supervision, M.G.D.G.; project administration, A.F.; funding acquisition, A.F. All authors have read and agreed to the published version of the manuscript.

Funding: This research was funded by the Italian Ministry of University and Research, project PON "SMEA", code PON03PE_00067_5.

Data Availability Statement: The data presented in this study are available on request from the corresponding author.

Conflicts of Interest: The authors declare no conflict of interest.

References

1. Kurz, R.; Brun, K.; Wollie, M. Degradation Effects on Industrial Gas Turbines. *J. Eng. Gas Turbines Power* **2009**, *131*, 062401. [CrossRef]
2. Ogiriki, E.; Li, Y.; Nikolaidis, T.; Isaiah, T.E.; Sule, G. Effect of Fouling, Thermal Barrier Coating Degradation and Film Cooling Holes Blockage on Gas Turbine Engine Creep Life. *Procedia CIRP* **2015**, *38*, 228–233. [CrossRef]
3. Masiol, M.; Harrison, R.M. Aircraft engine exhaust emissions and other airport-related contributions to ambient air pollution: A review. *Atmos. Environ.* **2014**, *95*, 409–455. [CrossRef]
4. Li, Z.; Zhong, S.; Lin, L. An aero-engine life-cycle maintenance policy optimization algorithm: Reinforcement learning approach. *Chin. J. Aeronaut.* **2019**, *32*, 2133–2150. [CrossRef]
5. Fornlöf, V.; Galar, D.; Syberfeldt, A.; Almgren, T. RUL estimation and maintenance optimization for aircraft engines: A system of system approach. *Int. J. Syst. Assur. Eng. Manag.* **2016**, *7*, 450–461. [CrossRef]
6. Kiyak, E. The Importance of Preventive Maintenance in terms of Reliability in Aviation Sector. In Proceedings of the 4th International Conference on Manufacturing Engineering, Quality and Production Systems, MEQAPS'11, Barcelona, Spain, 15–17 September 2011.
7. Almasi, A. Latest lessons learned, modern condition monitoring and advanced predictive maintenance for gas turbines. *Aust. J. Mech. Eng.* **2016**, *14*, 199–211. [CrossRef]
8. Rajamani, R.; Wang, J.; Jeong, K.Y. Condition-Based Maintenance for Aircraft Engines. *Turbo Expo Power Land Sea Air* **2004**, *41677*, 819–823. [CrossRef]
9. Jardine, A.K.S.; Lin, D.; Banjevic, D. A review on machinery diagnostics and prognostics implementing condition-based maintenance. *Mech. Syst. Signal Process.* **2006**, *20*, 1483–1510. [CrossRef]
10. Jimenez, J.J.M.; Schwartz, S.; Vingerhoeds, R.; Grabot, B.; Salaün, M. Towards multi-model approaches to predictive maintenance: A systematic literature survey on diagnostics and prognostics. *J. Manuf. Syst.* **2020**, *56*, 539–557. [CrossRef]
11. Atamuradov, V.; Camci, F.; Baskan, S.; Sevkli, M. Failure diagnostics for railway point machines using expert systems. In Proceedings of the IEEE International Symposium on Diagnostics for Electric Machines, Power Electronics and Drives, Cargèse, France, 31 August–3 September 2009; pp. 1–5.
12. Tahan, M.; Muhammad, M.; Karim, Z.A. A Framework for Intelligent Condition-based Maintenance of Rotating Equipment using Mechanical Condition Monitoring. *MATEC Web Conf.* **2014**, *13*, 05011. [CrossRef]
13. Ahmad, R.; Kamaruddin, S. An overview of time-based and condition-based maintenance in industrial application. *Comput. Ind. Eng.* **2012**, *63*, 135–149. [CrossRef]
14. Miller, J.L.; Kitaljevich, D. In-line oil debris monitor for aircraft engine condition assessment. In Proceedings of the 2000 IEEE Aerospace Conference, Big Sky, MN, USA, 18–25 March 2000; Volume 6, pp. 49–56.
15. Ao, C.; Qiao, B.; Liu, M.; Fu, S.; Yang, Z.; Chen, X. Dynamic Strain Reconstruction of Rotating Blades Based on Tip Timing and Response Transmissibility. *J. Eng. Gas Turbines Power* **2022**, *144*, 061011. [CrossRef]
16. Battiato, G.; Firrone, C.M.; Berruti, T.M. Forced response of rotating bladed disks: Blade Tip-Timing measurements. *Mech. Syst. Signal Process.* **2017**, *85*, 912–926. [CrossRef]
17. Xu, J.; Qiao, B.; Liu, M.; Fu, S.; Sun, Y.; Chen, X. Blade tip timing for monitoring crack propagation of rotor blades using Block-AOLS. *Mech. Syst. Signal Process.* **2022**, *181*, 109498. [CrossRef]
18. Ao, C.; Qiao, B.; Liu, M.; Zhu, W.; Zhu, Y.; Wang, Y.; Chen, X. Non-contact full-field dynamic strain reconstruction of rotating blades under multi-mode vibration. *Mech. Syst. Signal Process.* **2023**, *186*, 109840. [CrossRef]
19. Ao, C.; Qiao, B.; Chen, L.; Xu, J.; Liu, M.; Chen, X. Blade dynamic strain non-intrusive measurement using L1/2-norm regularization and transmissibility. *Measurement* **2022**, *190*, 110677. [CrossRef]
20. Mohamed, M.E.; Bonello, P.; Russhard, P. Determination of Simultaneous Steady-State Movements Using Blade Tip Timing Data. *J. Vib. Acoust.* **2019**, *142*, 011017. [CrossRef]
21. Williams, T.S. Advancing research efforts in biomimicry to develop nature-inspired materials, processes for space exploration and more efficient aircraft. In *Biomimicry for Aerospace*; Shyam, V., Eggermont, M., Hepp, A.F., Eds.; Elsevier: Amsterdam, The Netherlands, 2022; pp. 385–421.
22. Lurie-Luke, E. Product and technology innovation: What can biomimicry inspire? *Biotechnol. Adv.* **2014**, *32*, 1494–1505. [CrossRef]
23. Babbar, A.; Syrmos, V.L.; Ortiz, E.M.; Arita, M.M. Advanced diagnostics and prognostics for engine health monitoring. In Proceedings of the 2009 IEEE Aerospace Conference, Big Sky, MN, USA, 7–14 March 2009; pp. 1–10.
24. Wang, Z.; Zarader, J.L.; Argentieri, S. A novel aircraft engine fault diagnostic and prognostic system based on SVM. In Proceedings of the 2012 IEEE International Conference on Condition Monitoring and Diagnosis, Bali, Indonesia, 23–27 September 2012; pp. 723–728.
25. Zhang, B.; Zheng, K.; Huang, Q.; Feng, S.; Zhou, S.; Zhang, Y. Aircraft Engine Prognostics Based on Informative Sensor Selection and Adaptive Degradation Modeling with Functional Principal Component Analysis. *Sensors* **2020**, *20*, 920. [CrossRef]
26. Tahan, M.; Tsoutsanis, E.; Muhammad, M.; Karim, Z.A. Performance-based health monitoring, diagnostics and prognostics for condition-based maintenance of gas turbines: A review. *Appl. Energy* **2017**, *198*, 122–144. [CrossRef]
27. Marinai, L.; Probert, D.; Singh, R. Prospects for aero gas-turbine diagnostics: A review. *Appl. Energy* **2004**, *79*, 109–126. [CrossRef]
28. Rath, N.; Mishra, R.K.; Kushari, A. Aero engine health monitoring, diagnostics and prognostics for condition-based maintenance: An overview. *Int. J. Turbo Jet-Engines* **2022**, *5*. [CrossRef]

29. Clarkson, R.J.; Majewicz, E.J.; Mack, P. A re-evaluation of the 2010 quantitative understanding of the effects volcanic ash has on gas turbine engines. *Proc. Inst. Mech. Eng. Part G J. Aerosp. Eng.* **2016**, *230*, 2274–2291. [CrossRef]
30. DeRemer, J. Sand and Dust Erosion in Aircraft Gas Turbines. *J. Am. Soc. Nav. Eng.* **1950**, *62*, 505–511.
31. De Giorgi, M.G.; Campilongo, S.; Ficarella, A. Predictions of Operational Degradation of the Fan Stage of an Aircraft Engine Due to Particulate Ingestion. *J. Eng. Gas Turbines Power* **2015**, *137*, 052603-1. [CrossRef]
32. Hanachi, H.; Mechefske, C.; Liu, J.; Banerjee, A.; Chen, Y. Performance-Based Gas Turbine Health Monitoring, Diagnostics, and Prognostics: A Survey. *IEEE Trans. Reliab.* **2018**, *67*, 1340–1363. [CrossRef]
33. Meher-Homji, C.B.; Chaker, M.A.; Motiwala, H.M. Gas Turbine Performance Deterioration. In *Proceedings of the 30th Turbomachinery Symposium*; Texas A&M: College Station, TX, USA, 2001. [CrossRef]
34. Matthaiou, I.; Khandelwal, B.; Antoniadou, I. Vibration Monitoring of Gas Turbine Engines: Machine-Learning Approaches and Their Challenges. *Front. Built Environ.* **2017**, *3*, 54. [CrossRef]
35. Forest, F.; Cochard, Q.; Noyer, C.; Joncour, M.; Lacaille, J.; Lebbah, M.; Azzag, H. Large-scale Vibration Monitoring of Aircraft Engines from Operational Data using Self-organized Models. *Annu. Conf. PHM Soc.* **2020**, *12*, 11. [CrossRef]
36. Fabry, S.; Češkovič, M. Aircraft gas turbine engine vibration diagnostics. *MAD Mag. Aviat. Dev.* **2017**, *5*, 24. [CrossRef]
37. Powrie, H.; Novis, A. Gas path debris monitoring for F-35 Joint Strike Fighter propulsion system PHM. In Proceedings of the 2006 IEEE Aerospace Conference, Big Sky, MN, USA, 4–11 March 2006; p. 8.
38. Showalter, S.; Pingalkar, S.; Pasha, S. Oil debris monitoring in aerospace engines and helicopter transmissions. In Proceedings of the 2012 1st International Symposium on Physics and Technology of Sensors (ISPTS-1), Pune, India, 7–10 March 2012; pp. 1–2.
39. Fentaye, A.D.; Baheta, A.T.; Gilani, S.I.; Kyprianidis, K.G. A Review on Gas Turbine Gas-Path Diagnostics: State-of-the-Art Methods, Challenges and Opportunities. *Aerospace* **2019**, *6*, 83. [CrossRef]
40. Meher-Homji, C.B.; Chaker, M.; Bromley, A.F. The Fouling of Axial Flow Compressors: Causes, Effects, Susceptibility, and Sensitivity. *ASME Turbo Expo Power Land Sea Air* **2009**, *48852*, 571–590.
41. Kurz, R.; Brun, K. Fouling Mechanism in Axial Compressors. *ASME Turbo Expo Power Land Sea Air* **2011**, *54648*, 935–946. [CrossRef]
42. Diakunchak, I.S. Performance Deterioration in Industrial Gas Turbines. *J. Eng. Gas Turbines Power* **1992**, *114*, 161–168. [CrossRef]
43. Morini, M.; Pinelli, M.; Spina, P.R.; Venturini, M. Influence of Blade Deterioration on Compressor and Turbine Performance. *J. Eng. Gas Turbines Power* **2009**, *132*, 032401-1. [CrossRef]
44. Melino, F.; Morini, M.; Peretto, A.; Pinelli, M.; Spina, P.R. Compressor Fouling Modeling: Relationship Between Computational Roughness and Gas Turbine Operation Time. *J. Eng. Gas Turbines Power* **2012**, *134*, 052401. [CrossRef]
45. Igie, U.; Pilidis, P.; Fouflias, D.; Ramsden, K.; Laskaridis, P. Industrial Gas Turbine Performance: Compressor Fouling and On-Line Washing. *J. Turbomach.* **2014**, *136*, 101001. [CrossRef]
46. Meher-Homji, C.B.; Bromley, A. Gas Turbine Axial Compressor Fouling And Washing. In *Proceedings of the 33rd Turbomachinery Symposium*; Texas A&M: College Station, TX, USA, 2004. [CrossRef]
47. Boyce, M.P.; Gonzalez, F. A Study of On-Line and Off-Line Turbine Washing to Optimize the Operation of a Gas Turbine. *J. Eng. Gas Turbines Power* **2005**, *129*, 114–122. [CrossRef]
48. Yang, H.; Xu, H. The New Performance Calculation Method of Fouled Axial Flow Compressor. *Sci. World J.* **2014**, *2014*, e906151. [CrossRef]
49. Song, T.W.; Sohn, J.L.; Kim, T.S.; Kim, J.H.; Ro, S.T. An analytical approach to predicting particle deposit by fouling in the axial compressor of the industrial gas turbine. *Proc. Inst. Mech. Eng. Part A J. Power Energy* **2005**, *219*, 203–212. [CrossRef]
50. Kurz, R.; Musgrove, G.; Brun, K. Experimental Evaluation of Compressor Blade Fouling. *J. Eng. Gas Turbines Power* **2016**, *139*, 032601. [CrossRef]
51. Saravanamuttoo, H.I.H.; Lakshminarasimha, A.N. *A Preliminary Assessment of Compressor Fouling*; ASME: New York, NY, USA, 1985.
52. Aust, J.; Pons, D. Taxonomy of Gas Turbine Blade Defects. *Aerospace* **2019**, *6*, 58. [CrossRef]
53. Ellis, M.; Bojdo, N.; Filippone, A.; Clarkson, R. Monte Carlo Predictions of Aero-Engine Performance Degradation Due to Particle Ingestion. *Aerospace* **2021**, *8*, 146. [CrossRef]
54. Hamed, A.; Kuhn, T.P. Effects of Variational Particle Restitution Characteristics on Turbomachinery Erosion. *J. Eng. Gas Turbines Power* **1995**, *117*, 432–440. [CrossRef]
55. Salar, A.; Hosseini, M.; Zangmolk, B.; Sedigh, A.K. Improving Model-Based Gas Turbine Fault Diagnosis Using Multi-Operating Point Method. In Proceedings of the 2010 Fourth UKSim European Symposium on Computer Modeling and Simulation, Pisa, Italy, 17–19 November 2010; pp. 240–247.
56. Kurz, R.; Brun, K. Degradation in Gas Turbine Systems. *J. Eng. Gas Turbines Power* **2000**, *123*, 70–77. [CrossRef]
57. Grant, G.; Tabakoff, W. Erosion Prediction in Turbomachinery Resulting from Environmental Solid Particles. *J. Aircr.* **1975**, *12*, 471–478. [CrossRef]
58. Swadźba, L.; Formanek, B.; Gabriel, H.M.; Liberski, P.; Podolski, P. Erosion- and corrosion-resistant coatings for aircraft compressor blades. *Surf. Coat. Technol.* **1993**, *62*, 486–492. [CrossRef]
59. Wellman, R.G.; Nicholls, J.R. Erosion, corrosion and erosion–corrosion of EB PVD thermal barrier coatings. *Tribol. Int.* **2008**, *41*, 657–662. [CrossRef]

60. Chen, X.; He, M.Y.; Spitsberg, I.; Fleck, N.A.; Hutchinson, J.W.; Evans, A.G. Mechanisms Governing the High Temperature Erosion of Thermal Barrier Coatings Used in Gas Turbines. *Wear* **2004**, *256*, 735–746. [CrossRef]
61. Wellman, R.G.; Deakin, M.J.; Nicholls, J.R. The effect of TBC morphology on the erosion rate of EB PVD TBCs. *Wear* **2005**, *258*, 349–356. [CrossRef]
62. Wellman, R.G.; Nicholls, J.R. Some observations on erosion mechanisms of EB PVD TBCS. *Wear* **2000**, *242*, 89–96. [CrossRef]
63. Feuerstein, A.; Kleyman, A. Ti–N multilayer systems for compressor airfoil sand erosion protection. *Surf. Coat. Technol.* **2009**, *204*, 1092–1096. [CrossRef]
64. Wei, R.; Langa, E.; Rincon, C.; Arps, J.H. Deposition of thick nitrides and carbonitrides for sand erosion protection. *Surf. Coat. Technol.* **2006**, *201*, 4453–4459. [CrossRef]
65. Hamed, A.A.; Tabakoff, W.; Rivir, R.B.; Das, K.; Arora, P. Turbine Blade Surface Deterioration by Erosion. *J. Turbomach.* **2004**, *127*, 445–452. [CrossRef]
66. Casari, N.; Pinelli, M.; Suman, A.; di Mare, L.; Montomoli, F. EBFOG: Deposition, Erosion, and Detachment on High-Pressure Turbine Vanes. *J. Turbomach.* **2018**, *140*, 061001. [CrossRef]
67. Tabakoff, W. Compressor Erosion and Performance Deterioration. *J. Fluids Eng.* **1987**, *109*, 297–306. [CrossRef]
68. Hamed, A.; Tabakoff, W.C.; Wenglarz, R.V. Erosion and Deposition in Turbomachinery. *J. Propuls. Power* **2006**, *22*, 350–360. [CrossRef]
69. Tabakoff, W.; Lakshminarasimha, A.N.; Pasin, M. Simulation of Compressor Performance Deterioration Due to Erosion. *J. Turbomach.* **1990**, *112*, 78–83. [CrossRef]
70. Wilcox, M.; Kurz, R.; Brun, K. Successful Selection And Operation Of Gas Turbine Inlet Filtration Systems. In *Proceedings of the 40th Turbomachinery Symposium*; Texas A&M University: College Station, TX, USA, 2011. [CrossRef]
71. Lai, G.Y. Hot Corrosion in Gas Turbines. In *High-Temperature Corrosion and Materials Applications*; ASM International: Materials Park, OH, USA, 2007. [CrossRef]
72. Salehnasab, B.; Poursaeidi, E.; Mortazavi, A.; Farokhian, G.H. Hot corrosion failure in the first stage nozzle of a gas turbine engine. *Eng. Fail. Anal.* **2015**, *60*, 316–325. [CrossRef]
73. Czaban, M. Aircraft Corrosion—Review of Corrosion Processes and its Effects in Selected Cases. *Fatigue Aircr. Struct.* **2018**, *2018*, 5–20. [CrossRef]
74. Hocko, M. Gas corrosion of parts of turbofan military engine gas turbine. *AIP Conf. Proc.* **2021**, *2323*, 060005.
75. Kim, J.; Le, M.; Lee, J.; Hwang, Y.H. Eddy Current Testing and Evaluation of Far-Side Corrosion Around Rivet in Jet-Engine Intake of Aging Supersonic Aircraft. *J. Nondestruct. Eval.* **2014**, *33*, 471–480. [CrossRef]
76. Kant, R.; Chauhan, P.S.; Bhatt, G.; Bhattacharya, S. Corrosion Monitoring and Control in Aircraft: A Review. In *Sensors for Automotive and Aerospace Applications*; Bhattacharya, S., Agarwal, A.K., Prakash, O., Singh, S., Eds.; Springer: Singapore, 2019; pp. 39–53.
77. Van Roode, M.; Hsu, L. Evaluation of the hot corrosion protection of coatings for turbine hot section components. *Surf. Coat. Technol.* **1989**, *37*, 461–481. [CrossRef]
78. Varelis, A.G. Technoeconomic Study of Engine Deterioration and Compressor Washing for Military Gas Turbine Engines. Ph.D. Thesis, Cranfield University, Cranfield, UK, 2008.
79. Piollet, E.; Nyssen, F.; Batailly, A. Blade/casing rubbing interactions in aircraft engines: Numerical benchmark and design guidelines based on NASA rotor 37. *J. Sound Vib.* **2019**, *460*, 114878. [CrossRef]
80. Kurz, R.; Brun, K. Gas Turbine Tutorial—Maintenance and Operating Practices Effects On Degradation And Life. In *Proceedings of the 36th Turbomachinery Symposium*; Texas A&M University: College Station, TX, USA, 2007. [CrossRef]
81. Xuan, H.; Zhang, N.; Lu, B.; Chen, L.; Hong, W. Investigation of high-speed abrasion behavior of an abradable seal rubber in aero-engine fan application. *Chin. J. Aeronaut.* **2017**, *30*, 1615–1623. [CrossRef]
82. Zaita, A.V.; Buley, G.; Karlsons, G. Performance Deterioration Modeling in Aircraft Gas Turbine Engines. *J. Eng. Gas Turbines Power* **1998**, *120*, 344–349. [CrossRef]
83. Hussin, R.; Ismail, N.; Mustapa, S. A study of foreign object damage (FOD) and prevention method at the airport and aircraft maintenance area. *IOP Conf Ser. Mater. Sci. Eng.* **2016**, *152*, 012038. [CrossRef]
84. Meher-Homji, C.B.; Matthews, T.; Pelagotti, A.; Weyermann, H.P. Gas Turbines and Turbocompressors For LNG Service. In *Proceedings of the 36th Turbomachinery Symposium*; Texas A&M University: College Station, TX, USA, 2007. [CrossRef]
85. Yu, B.; Ke, H.; Shen, E.; Zhang, T. A review of blade tip clearance–measuring technologies for gas turbine engines. *Meas. Control* **2020**, *53*, 339–357. [CrossRef]
86. Wisler, D.C. Loss Reduction in Axial-Flow Compressors Through Low-Speed Model Testing. *J. Eng. Gas Turbines Power* **1985**, *107*, 354–363. [CrossRef]
87. Chivers, J. A technique for the measurement of blade tip clearance in a gas turbine. In *25th Joint Propulsion Conference*; American Institute of Aeronautics and Astronautics: Reston, VA, USA, 1989. [CrossRef]
88. MacIsaac, B.D. *Engine Performance and Health Monitoring Models Using Steady State and Transient Prediction Methods*; DTIC Document; DTIC: Fort Belvoir, VA, USA, 1992.
89. Frith, P.C. The Effect of Compressor Rotor Tip Crops on Turboshaft Engine Performance. *Turbo Expo Power Land Sea Air* **2015**, *78941*, V002T02A005. [CrossRef]
90. Gourdain, N.; Wlassow, F.; Ottavy, X. Effect of Tip Clearance Dimensions and Control of Unsteady Flows in a Multi-Stage High-Pressure Compressor. *J. Turbomach.* **2012**, *134*, 051005. [CrossRef]

91. Fu, Z.; Wang, Y.; Jiang, X.; Wei, D. Tip Clearance Effects on Aero-elastic Stability of Axial Compressor Blades. *J. Eng. Gas Turbines Power* **2014**, *137*, 012501-1. [CrossRef]
92. Han, L.; Wei, D.; Wang, Y.; Jiang, X.; Zhang, X. Analysis Method of Nonsynchronous Vibration and Influence of Tip Clearance Flow Instabilities on Nonsynchronous Vibration in an Axial Transonic Compressor Rotor. *J. Turbomach.* **2021**, *143*, 111014. [CrossRef]
93. Stapelfeldt, S.; Brandstetter, C. Non-synchronous vibration in axial compressors: Lock-in mechanism and semi-analytical model. *J. Sound Vib.* **2020**, *488*, 115649. [CrossRef]
94. Li, Z.; Wang, Y.; Qiao, B.; Wen, B.; Chen, F. Experimental investigation of aeroelastic instabilities in an aeroengine fan: Using acoustic measurements. *Aerosp. Sci. Technol.* **2022**, *130*, 107927. [CrossRef]
95. Binghui, J.; Lei, H.; Yong, F.; Jinlong, Z.; Gang, Q. The development of aero-engine tip-clearance measurement technology: A simple review. In Proceedings of the 2017 13th IEEE International Conference on Electronic Measurement Instruments (ICEMI), Yangzhou, China, 20–23 October 2017; pp. 565–570.
96. Rani, S.; Agrawal, A.K.; Rastogi, V. Failure analysis of a first stage IN738 gas turbine blade tip cracking in a thermal power plant. *Case Stud. Eng. Fail. Anal.* **2017**, *8*, 1–10. [CrossRef]
97. Grassart, P. Monitoring of the Lubrication System of an Aircraft Engine through a Prognostic and Health Monitoring Approach. Master's Thesis, KTH School of Industrial Engineering and Management, Stockholm, Sweden, 2015.
98. Garg, S.; Schadow, K.; Horn, W.; Pfoertner, H.; Stiharu, I. Sensor and Actuator Needs for More Intelligent Gas Turbine Engines. *Turbo Expo Power Land Sea Air* **2010**, *43987*, 155–167. [CrossRef]
99. Hua, H.; Zhang, Z.; Feng, H. Research Status and Method of Aviation Sensor Performance Evaluation. *J. Phys. Conf. Ser.* **2021**, *1769*, 012050. [CrossRef]
100. Simon, D.L.; Rinehart, A.W. Sensor Selection for Aircraft Engine Performance Estimation and Gas Path Fault Diagnostics. *J. Eng. Gas Turbines Power* **2016**, *138*, 071201. [CrossRef]
101. Pourbabaee, B.; Meskin, N.; Khorasani, K. Sensor Fault Detection, Isolation, and Identification Using Multiple-Model-Based Hybrid Kalman Filter for Gas Turbine Engines. *IEEE Trans. Control Syst. Technol.* **2016**, *24*, 1184–1200. [CrossRef]
102. Sadough Vanini, Z.N.; Meskin, N.; Khorasani, K. Multiple-Model Sensor and Components Fault Diagnosis in Gas Turbine Engines Using Autoassociative Neural Networks. *J. Eng. Gas Turbines Power* **2015**, *136*, 091603. [CrossRef]
103. Kramer, M.A. Autoassociative neural networks. *Comput. Chem. Eng.* **1992**, *16*, 313–328. [CrossRef]
104. Abernathy, R.B.; Powell, B.D.; Colbert, D.L.; Sanders, D.G.; Thompson, J.W., Jr. *Handbook, Uncertainty in Gas Turbine Measurements*; DTIC Document; DTIC: Fort Belvoir, VA, USA, 1973.
105. Qiu, H.; Eklund, N.; Iyer, N.; Hu, X. Evaluation of filtering techniques for aircraft engine condition monitoring and diagnostics. In Proceedings of the 2008 International Conference on Prognostics and Health Management, Denver, CO, USA, 6–9 October 2008. [CrossRef]
106. Jerath, K.; Brennan, S.; Lagoa, C. Bridging the gap between sensor noise modeling and sensor characterization. *Measurement* **2018**, *116*, 350–366. [CrossRef]
107. Cho, Y.H.; Song, M. Noise reduction of FBG sensor signal by using a wavelet transform. In *Optical Sensors 2011; and Photonic Crystal Fibers V*; SPIE: Bellingham, WA, USA, 2011; pp. 380–385.
108. Adochiei, I.; Felix Constantin, A.; Radu, O.; Grigorie, T.L. Inertial Sensor Signals Denoising with Wavelet Transform. *Incas Bull.* **2015**, *7*, 57–64.
109. Zhang, X.; Wang, Y.; Han, R.P.S. Wavelet transform theory and its application in EMG signal processing. In Proceedings of the 2010 Seventh International Conference on Fuzzy Systems and Knowledge Discovery, Yantai, China, 10–12 August 2010; pp. 2234–2238.
110. Khalid, S.; Khalil, T.; Nasreen, S. A survey of feature selection and feature extraction techniques in machine learning. In Proceedings of the 2014 Science and Information Conference, London, UK, 27–29 August 2014; pp. 372–378.
111. Buchaiah, S.; Shakya, P. Bearing fault diagnosis and prognosis using data fusion based feature extraction and feature selection. *Measurement* **2022**, *188*, 110506. [CrossRef]
112. Anowar, F.; Sadaoui, S.; Selim, B. Conceptual and empirical comparison of dimensionality reduction algorithms (PCA, KPCA, LDA, MDS, SVD, LLE, ISOMAP, LE, ICA, t-SNE). *Comput. Sci. Rev.* **2021**, *40*, 100378. [CrossRef]
113. De Giorgi, M.G.; Strafella, L.; Menga, N.; Ficarella, A. Development of a combined Artificial Neural Network and Principal Component Analysis technique for Engine Health Monitoring. *IOP Conf.Ser. Mater. Sci. Eng.* **2022**, *1226*, 012035. [CrossRef]
114. Ji, S.; Han, X.; Hou, Y.; Song, Y.; Du, Q. Remaining Useful Life Prediction of Airplane Engine Based on PCA–BLSTM. *Sensors* **2020**, *20*, 4537. [CrossRef]
115. De Giorgi, M.G.; Strafella, L.; Menga, N.; Ficarella, A. Intelligent Combined Neural Network and Kernel Principal Component Analysis Tool for Engine Health Monitoring Purposes. *Aerospace* **2022**, *9*, 118. [CrossRef]
116. Zhang, Y.; Liu, C. Face recognition using kernel principal component analysis and genetic algorithms. In Proceedings of the 12th IEEE Workshop on Neural Networks for Signal Processing, Martigny, Switzerland, 4–6 September 2002; pp. 337–343.
117. Cui, J.; Li, G.; Yu, M.; Jiang, L.; Lin, Z. Aero-engine Fault Diagnosis Based on Kernel Principal Component Analysis and Wavelet Neural Network. In Proceedings of the 2019 Chinese Control And Decision Conference (CCDC), Nanchang, China, 3–5 June 2019; pp. 451–456.
118. Zhou, Y.; Yan, S.; Ren, Y.; Liu, S. Rolling bearing fault diagnosis using transient-extracting transform and linear discriminant analysis. *Measurement* **2021**, *178*, 109298. [CrossRef]

119. Chen, J.; Chen, S.; Liu, Z.; Luo, C.; Jing, Z.; Xu, Q. Health Monitoring of Landing Gear Retraction/Extension System Based on Optimized Fuzzy C-Means Algorithm. *IEEE Access* **2020**, *8*, 219611–219621. [CrossRef]
120. Remadna, I.; Terrissa, S.L.; Zemouri, R.; Ayad, S.; Zerhouni, N. Unsupervised Feature Reduction Techniques with Bidirectional GRU Neural Network for Aircraft Engine RUL Estimation. In *Advanced Intelligent Systems for Sustainable Development (AI2SD'2019)*; Ezziyyani, M., Ed.; Springer: Cham, Switzerland, 2020; pp. 496–506.
121. Sun, C.; Wang, P.; Yan, R.; Gao, R.X.; Chen, X. Machine health monitoring based on locally linear embedding with kernel sparse representation for neighborhood optimization. *Mech. Syst. Signal Process.* **2019**, *114*, 25–34. [CrossRef]
122. Zhang, Y.; Li, B.; Wang, Z.; Wang, W.; Wang, L. Fault diagnosis of rotating machine by isometric feature mapping. *J. Mech. Sci. Technol.* **2013**, *27*, 3215–3221. [CrossRef]
123. Qiu, G.; Huang, S.; Chen, Y. Automatic segmentation and prognostic method of a turbofan engine using manifold learning and spectral clustering algorithms. *Adv. Mech. Eng.* **2017**, *9*, 1687814017722712. [CrossRef]
124. Wen, Z.; Zuo, H.; Pecht, M.G. Electrostatic Monitoring of Gas Path Debris for Aero-engines. *IEEE Trans. Reliab.* **2011**, *60*, 33–40. [CrossRef]
125. Widodo, A.; Yang, B.S.; Han, T. Combination of independent component analysis and support vector machines for intelligent faults diagnosis of induction motors. *Expert Syst. Appl.* **2007**, *32*, 299–312. [CrossRef]
126. Xu, Y.; Hou, W.; Li, W.; Zheng, N. Aero-Engine Gas-path Fault Diagnosis Based on Spatial Structural Characteristics of QAR Data. In Proceedings of the 2018 Annual Reliability and Maintainability Symposium (RAMS), Reno, NV, USA, 22–25 January 2018; pp. 1–7.
127. Li, B.; Zhao, Y.P.; Chen, Y.B. Unilateral alignment transfer neural network for fault diagnosis of aircraft engine. *Aerosp. Sci. Technol.* **2021**, *118*, 107031. [CrossRef]
128. Pacini, G.C.; Colucci, D.; Baudron, F.; Righi, E.; Corbeels, M.; Tittonell, P. Combining multi-dimensional scaling and cluster analysis to describe the diversity of rural households. *Exp. Agric.* **2014**, *50*, 376–397. [CrossRef]
129. Gerdes, M.; Scholz, D.; Galar, D. Effects of condition-based maintenance on costs caused by unscheduled maintenance of aircraft. *J. Qual. Maint. Eng.* **2016**, *22*, 394–417. [CrossRef]
130. Engel, S.J.; Gilmartin, B.J.; Bongort, K.; Hess, A. Prognostics, the real issues involved with predicting life remaining. In Proceedings of the 2000 IEEE Aerospace Conference Proceedings, Big Sky, MT, USA, 25 March 2000; IEEE: Piscataway, NJ, USA, 2000; Volume 6, pp. 457–469.
131. Baraldi, P.; Cadini, F.; Mangili, F.; Zio, E. Model-based and data-driven prognostics under different available information. *Probabilistic Eng. Mech.* **2013**, *32*, 66–79. [CrossRef]
132. Xu, G.; Liu, M.; Wang, J.; Ma, Y.; Wang, J.; Li, F.; Shen, W. Data-Driven Fault Diagnostics and Prognostics for Predictive Maintenance: A Brief Overview. In Proceedings of the 2019 IEEE 15th International Conference on Automation Science and Engineering (CASE), Vancouver, BC, Canada, 22–26 August 2019; pp. 103–108.
133. Ntantis, E.L.; Botsaris, P. Diagnostic methods for an aircraft engine performance. *J. Eng. Sci. Technol. Rev.* **2015**, *8*, 64–72. [CrossRef]
134. Simon, D. A comparison of filtering approaches for aircraft engine health estimation. *Aerosp. Sci. Technol.* **2008**, *12*, 276–284. [CrossRef]
135. Kong, C. Review on Advanced Health Monitoring Methods for Aero Gas Turbines using Model Based Methods and Artificial Intelligent Methods. *Int. J. Aeronaut. Space Sci.* **2014**, *15*, 123–137. [CrossRef]
136. Urban, L.A. Gas Path Analysis Applied to Turbine Engine Condition Monitoring. *J. Aircr.* **1973**, *10*, 400–406. [CrossRef]
137. Escher, P.C. Pythia: An Object-Orientated Gas Path Analysis Computer Program for General Applications. Ph.D. Thesis, Cranfield University, Cranfield, UK, 1995.
138. Urban, L.A. *Gas Turbine Engine Parameter Interrelationships*; Hamilton Standard Division of United Aircraft Corporation: Windsor Locks, CT, USA, 1969.
139. Saravanamuttoo, H.I.H.; MacIsaac, B.D. Thermodynamic Models for Pipeline Gas Turbine Diagnostics. *J. Eng. Power* **1983**, *105*, 875–884. [CrossRef]
140. Aker, G.F.; Saravanamuttoo, H.I.H. Predicting Gas Turbine Performance Degradation Due to Compressor Fouling Using Computer Simulation Techniques. *J. Eng. Gas Turbines Power* **1989**, *111*, 343–350. [CrossRef]
141. Ogaji, S.O.T.; Sampath, S.; Singh, R.; Probert, S.D. Parameter selection for diagnosing a gas-turbine's performance-deterioration. *Appl. Energy* **2002**, *73*, 25–46. [CrossRef]
142. Donaghy, M.J. Gas Path Analysis: Fault Diagnosis Using DETEM. Ph.D. Thesis, Cranfield Institute of Technology, School of Mechanical Engineering, Cranfield, UK, 1991.
143. Verbist, M.L.; Visser, W.P.J.; van Buijtenen, J.P.; Duivis, R. Gas Path Analysis on KLM In-Flight Engine Data. *Turbo Expo Power Land Sea Air* **2011**, *54631*, 149–157.
144. Zhou, H.; Ying, Y.; Li, J.; Jin, Y. Long-short term memory and gas path analysis based gas turbine fault diagnosis and prognosis. *Adv. Mech. Eng.* **2021**, *13*, 16878140211037768. [CrossRef]
145. Kalman, R.E. A New Approach to Linear Filtering and Prediction Problems. *J. Basic Eng.* **1960**, *82*, 35–45. [CrossRef]
146. Giron-Sierra, J. Kalman Filter, Particle Filter and Other Bayesian Filters. *Digit. Signal Process. Matlab Ex.* **2017**, *3*, 3–148.
147. Valade, A.; Acco, P.; Grabolosa, P.; Fourniols, J.Y. A Study about Kalman Filters Applied to Embedded Sensors. *Sensors* **2017**, *17*, 2810. [CrossRef] [PubMed]
148. Volponi, A.J.; DePold, H.; Ganguli, R.; Daguang, C. The Use of Kalman Filter and Neural Network Methodologies in Gas Turbine Performance Diagnostics: A Comparative Study. *J. Eng. Gas Turbines Power* **2003**, *125*, 917–924. [CrossRef]

149. Kobayashi, T.; Simon, D. Application of a Bank of Kalman Filters for Aircraft Engine Fault Diagnostics. *Turbo Expo Power Land Sea Air* **2003**, *36843*, 461–470. [CrossRef]
150. Kobayashi, T.; Simon, D. Hybrid Kalman Filter Approach for Aircraft Engine In-Flight Diagnostics: Sensor Fault Detection Case. *J. Eng. Gas Turbines Power* **2006**, *129*, 746–754. [CrossRef]
151. Kobayashi, T.; Simon, D.L. Evaluation of an Enhanced Bank of Kalman Filters for In-Flight Aircraft Engine Sensor Fault Diagnostics. *J. Eng. Gas Turbines Power* **2005**, *127*, 497–504. [CrossRef]
152. Xue, W.; Guo, Y.; Zhang, X. A Bank of Kalman Filters and a Robust Kalman Filter Applied in Fault Diagnosis of Aircraft Engine Sensor/Actuator. In Proceedings of the Second International Conference on Innovative Computing, Informatio and Control (ICICIC 2007), Kumamoto, Japan, 5–7 September 2007; p. 10.
153. Borguet, S.; Léonard, O. Coupling principal component analysis and Kalman filtering algorithms for on-line aircraft engine diagnostics. *Control Eng. Pract.* **2009**, *17*, 494–502. [CrossRef]
154. Dewallef, P.; Romessis, C.; Léonard, O.; Mathioudakis, K. Combining Classification Techniques With Kalman Filters for Aircraft Engine Diagnostics. *J. Eng. Gas Turbines Power* **2004**, *128*, 281–287. [CrossRef]
155. Lu, F.; Wang, Y.; Huang, J.; Huang, Y.; Qiu, X. Fusing unscented Kalman filter for performance monitoring and fault accommodation in gas turbine. *Proc. Inst. Mech. Eng. Part G J. Aerosp. Eng.* **2018**, *232*, 556–570. [CrossRef]
156. Haykin, S. *Kalman Filtering and Neural Networks*; John Wiley & Sons: Hoboken, NJ, USA, 2004.
157. Luppold, R.; Roman, J.; Gallops, G.; Kerr, L. Estimating in-flight engine performance variations using Kalman filter concepts. In *Proceedings of the 25th Joint Propulsion Conference*; American Institute of Aeronautics and Astronautics: Monterey, CA, USA, 1989. [CrossRef]
158. Li, Q.; Li, R.; Ji, K.; Dai, W. Kalman Filter and Its Application. In Proceedings of the 2015 8th International Conference on Intelligent Networks and Intelligent Systems (ICINIS), Tianjin, China, 1–3 November 2015; pp. 74–77.
159. Chen, J.; Ma, C.; Song, D.; Xu, B. Failure prognosis of multiple uncertainty system based on Kalman filter and its application to aircraft fuel system. *Adv. Mech. Eng.* **2016**, *8*, 1687814016671445. [CrossRef]
160. Lu, F.; Ju, H.; Huang, J. An improved extended Kalman filter with inequality constraints for gas turbine engine health monitoring. *Aerosp. Sci. Technol.* **2016**, *58*, 36–47. [CrossRef]
161. Goldberd, D.E. *Genetic Algorithms in Search, Optimization and Machine Learning*; Addison–Wesley: Boston, MA, USA, 1989.
162. Tang, K.S.; Man, K.F.; Kwong, S.; He, Q. Genetic algorithms and their applications. *IEEE Signal Process. Mag.* **1996**, *13*, 22–37. [CrossRef]
163. Chakroborty, P. Genetic Algorithms for Optimal Urban Transit Network Design. *Comput.-Aided Civ. Infrastruct. Eng.* **2003**, *18*, 184–200. [CrossRef]
164. Li, Y.G. Performance-analysis-based gas turbine diagnostics: A review. *Proc. Inst. Mech. Eng. Part A J. Power Energy* **2002**, *216*, 363–377. [CrossRef]
165. Sampath, S.; Ogaji, S.; Singh, R.; Probert, D. Engine-fault diagnostics: An optimisation procedure. *Appl. Energy* **2002**, *73*, 47–70. [CrossRef]
166. Bodenhofer, U. *Genetic Algorithms: Theory and Applications*; Fuzzy Logic Laboratorium Linz-Hagenberg: Winter, Germany, 1999.
167. Schmitt, L.M. Theory of genetic algorithms. *Theor. Comput. Sci.* **2001**, *259*, 1–61. [CrossRef]
168. Kobayashi, T.; Simon, D. A Hybrid Neural Network-Genetic Algorithm Technique for Aircraft Engine Performance Diagnostics. *J. Propuls. Power* **2001**, *21*, 751–758. [CrossRef]
169. Li, Y.G. Diagnostics of power setting sensor fault of gas turbine engines using genetic algorithm. *Aeronaut. J.* **2017**, *121*, 1109–1130. [CrossRef]
170. Da Costa, F.P.; Domingues, P.H.L.S.P.; Freire, R.Z.; Coelho, L.S.; Tavakolpour-Saleh, A.R.; Ayala, H.V.H. Genetic Algorithm for Topology Optimization of an Artificial Neural Network Applied to Aircraft Turbojet Engine Identification. In Proceedings of the 2019 IEEE Congress on Evolutionary Computation (CEC), Wellington, New Zealand, 10–13 June 2019; pp. 1095–1101.
171. Gerdes, M.; Galar, D.; Scholz, D. Genetic algorithms and decision trees for condition monitoring and prognosis of A320 aircraft air conditioning. *Insight Non-Destr. Test. Cond. Monit.* **2017**, *59*, 424–433. [CrossRef]
172. Zhang, Z. Artificial Neural Network. In *Multivariate Time Series Analysis in Climate and Environmental Research*; Zhang, Z., Ed.; Springer: Cham, Switzerland, 2018; pp. 1–35.
173. Bebis, G.; Georgiopoulos, M. Feed-forward neural networks. *IEEE Potentials* **1994**, *13*, 27–31. [CrossRef]
174. Svozil, D.; Kvasnicka, V.; Pospichal, J. Introduction to multi-layer feed-forward neural networks. *Chemom. Intell. Lab. Syst.* **1997**, *39*, 43–62. [CrossRef]
175. Wang, S.C. Artificial Neural Network. In *Interdisciplinary Computing in Java Programming*; Wang, S.C., Ed.; Springer: Boston, MA, USA, 2003; pp. 81–100.
176. Medsker, L.; Jain, L.C. *Recurrent Neural Networks: Design and Applications*; CRC Press: Boca Raton, FL, USA, 1999.
177. Mandic, D.; Chambers, J. *Recurrent Neural Networks for Prediction: Learning Algorithms, Architectures and Stability*; Wiley: Chichester, UK, 2001.
178. De Giorgi, M.G.; Campilongo, S.; Ficarella, A. A diagnostics tool for aero-engines health monitoring using machine learning technique. *Energy Procedia* **2018**, *148*, 860–867. [CrossRef]

179. Alam, M.M.; Bodruzzaman, M.; Zein-Sabatto, M.S. Online prognostics of aircraft turbine engine component's remaining useful life (RUL). In Proceedings of the IEEE SOUTHEASTCON 2014, Lexington, KY, USA, 14–16 March 2014; IEEE: Piscataway, NJ, USA, 2014; pp. 1–6.
180. Sampath, S. Fault Diagnostics for Advanced Cycle Marine Gas Turbine Using Genetic Algorithm. Ph.D. Thesis, Cranfield University, Cranfield, UK, 2003.
181. Lauría, E.J.M.; Duchessi, P.J. A Bayesian Belief Network for IT implementation decision support. *Decis. Support Syst.* **2006**, *42*, 1573–1588. [CrossRef]
182. Breese, J.S.; Horvitz, E.J.; Peot, M.A.; Gay, R.; Quentin, G. Automated Decision-Analytic Diagnosis of Thermal Performance in Gas Turbines. *Turbo Expo Power Land Sea Air* **2015**, *78972*, V005T15A015. [CrossRef]
183. Romessis, C.; Mathioudakis, K. Bayesian Network Approach for Gas Path Fault Diagnosis. *J. Eng. Gas Turbines Power* **2004**, *128*, 64–72. [CrossRef]
184. Mast, T.A.; Reed, A.T.; Yurkovich, S.; Ashby, M.; Adibhatla, S. Bayesian belief networks for fault identification in aircraft gas turbine engines. In Proceedings of the 1999 IEEE International Conference on Control Applications, Kohala Coast, HI, USA, 22–27 August 1999; IEEE: Piscataway, NJ, USA, 1999; Volume 1, pp. 39–44.
185. Ferreiro, S.; Arnaiz, A.; Sierra, B.; Irigoien, I. Application of Bayesian networks in prognostics for a new Integrated Vehicle Health Management concept. *Expert Syst. Appl.* **2012**, *39*, 6402–6418. [CrossRef]
186. Ortolano, L.; Perman, C.D. Software for Expert Systems Development. *J. Comput. Civ. Eng.* **1987**, *1*, 225–240. [CrossRef]
187. Collinge, K.; Schoff, K. *TEXMAS—An Expert System for Gas Turbine Engine Diagnosis and More*; SAE: Warrendale, PA, USA, 1987.
188. Hamilton, T.P. HELIX: A helicopter diagnostic system based on qualitative physics. *Artif. Intell. Eng.* **1988**, *3*, 141–150. [CrossRef]
189. Jellison, T.; Frenster, J.; Pratt, N.; Dehoff, R. XMAN—A tool for automated jet engine diagnostics. In Proceedings of the 23rd Joint Propulsion Conference, San Diego, CA, USA, 29 June–2 July 1987; American Institute of Aeronautics and Astronautics: Reston, VA, USA, 1987. [CrossRef]
190. Abadir, M.S. TIGER: Testability insertion guidance expert system. In Proceedings of the 1989 IEEE International Conference on Computer-Aided Design. Digest of Technical Papers, Santa Clara, CA, USA, 5–9 November 1989; IEEE: Piscataway, NJ, USA, 1989; pp. 562–565.
191. Zadeh, L.A. Outline of a New Approach to the Analysis of Complex Systems and Decision Processes. *IEEE Trans. Syst. Man Cybern.* **1973**, *3*, 28–44. [CrossRef]
192. Zadeh, L.A. Fuzzy sets. *Inf. Control* **1965**, *8*, 338–353. [CrossRef]
193. Ross, T.J. *Fuzzy Logic with Engineering Applications*; John Wiley and Sons: Hoboken, NJ, USA, 2009.
194. Marinai, L. Gas-Path Diagnostics and Prognostics for Aero-Engines Using Fuzzy Logic and Time Series Analysis. Ph.D. Thesis, Cranfield University, Cranfield, UK, 2004.
195. Ogaji, S.O.T.; Marinai, L.; Sampath, S.; Singh, R.; Prober, S.D. Gas-turbine fault diagnostics: A fuzzy-logic approach. *Appl. Energy* **2005**, *82*, 81–89. [CrossRef]
196. Ganguli, R. Application of Fuzzy Logic for Fault Isolation of Jet Engines. *J. Eng. Gas Turbines Power* **2003**, *125*, 617–623. [CrossRef]
197. Ganguli, R. Fuzzy Logic Intelligent System for Gas Turbine Module and System Fault Isolation. *J. Propuls. Power* **2002**, *18*, 440–447. [CrossRef]
198. Marinai, L.; Singh, R. A Fuzzy Logic Approach to Gas Path Diagnostics in Aero-engines. In *Computational Intelligence in Fault Diagnosis*; Springer: Cham, Switzerland, 2006. [CrossRef]
199. Gayme, D.; Menon, S.; Ball, C.; Mukavetz, D.; Nwadiogbu, E. Fault diagnosis in gas turbine engines using fuzzy logic. In Proceedings of the SMC'03, IEEE International Conference on Systems, Man and Cybernetics. Conference Theme—System Security and Assurance, Washington, DC, USA, 8 October 2003; IEEE: Piscataway, NJ, USA, 2003; Volume 4, pp. 3756–3762.
200. Zhou, D.; Zhang, H.; Weng, S. A New Gas Path Fault Diagnostic Method of Gas Turbine Based on Support Vector Machine. *J. Eng. Gas Turbines Power* **2015**, *137*, 102605. [CrossRef]
201. Saimurugan, M.; Ramachandran, K.I.; Sugumaran, V.; Sakthivel, N.R. Multi component fault diagnosis of rotational mechanical system based on decision tree and support vector machine. *Expert Syst. Appl.* **2011**, *38*, 3819–3826. [CrossRef]
202. Fentaye, A.D.; Ul-Haq Gilani, S.I.; Baheta, A.T.; Li, Y.G. Performance-based fault diagnosis of a gas turbine engine using an integrated support vector machine and artificial neural network method. *Proc. Inst. Mech. Eng. Part A J. Power Energy* **2019**, *233*, 786–802. [CrossRef]
203. Huang, C.L.; Wang, C.J. A GA-based feature selection and parameters optimizationfor support vector machines. *Expert Syst. Appl.* **2006**, *31*, 231–240. [CrossRef]
204. Tian, F.; Li, W.J.; Feng, Z.G.; Zhang, R. Fault Diagnosis for Aircraft Engine Based on SVM Multiple Classifiers Fusion. *Appl. Mech. Mater.* **2013**, *433*, 607–611. [CrossRef]
205. De Pádua Moreira, R.; Nascimento, C.L. Prognostics of aircraft bleed valves using a SVM classification algorithm. In Proceedings of the 2012 IEEE Aerospace Conference, Big Sky, MT, USA, 3–10 March 2012; IEEE: Piscataway, NJ, USA, 2012; pp. 1–8.